Biogeosciences Discuss., 11, 6069–6117, 2014
www.biogeosciences-discuss.net/11/6069/2014/
doi:10.5194/bgd-11-6069-2014
© Author(s) 2014. CC Attribution 3.0 License.

Biogeosciences Discussions Open Access

This discussion paper is/has been under review for the journal Biogeosciences (BG).
Please refer to the corresponding final paper in BG if available.

Atmospheric inversion of the surface carbon flux with consideration of the spatial distributions of US crop production and consumption

J. M. Chen[1,2], J. W. Fung[2], G. Mo[2], F. Deng[3], and T. O. West[4]

[1]International Institute of Earth System Science Nanjing University Nanjing, Jiangsu, China
[2]Department of Geography & Planning, University of Toronto, Toronto, Ontario, M5S 3G3, Canada
[3]Department of Physics University of Toronto, Toronto, Ontario, M5S 3G3, Canada
[4]Joint Global Change Research Institute, Pacific Northwest National Laboratory, College Park, Maryland, USA

Received: 26 November 2013 – Accepted: 10 March 2014 – Published: 29 April 2014

Correspondence to: J. M. Chen (chenj@geog.utoronto.ca)

Published by Copernicus Publications on behalf of the European Geosciences Union.

Abstract

In order to improve quantification of the spatial distribution of carbon sinks and sources in the conterminous USA, we conduct a nested global atmospheric inversion with consideration of the spatial information of crop production and consumption. Spatially distributed county-level cropland net primary productivity, harvested biomass, soil carbon change, and human and livestock consumption data over the conterminous USA are used for this purpose. Time-dependent Bayesian synthesis inversions are conducted based on CO_2 observations at 210 stations to infer CO_2 fluxes globally at monthly time steps with a nested focus on 30 regions in North America. Prior land surface carbon fluxes are first generated using a biospheric model, and the inversions are constrained using prior fluxes with and without adjustments for crop production and consumption over the 2002–2007 period. After these adjustments, the inverted regional carbon sink in the US Midwest increases from $0.25 \pm 0.03\,\mathrm{Pg\,C\,yr^{-1}}$ to $0.42 \pm 0.13\,\mathrm{Pg\,C\,yr^{-1}}$, whereas the large sink in the US Southeast forest region is weakened from $0.41 \pm 0.12\,\mathrm{Pg\,C\,yr^{-1}}$ to $0.29 \pm 0.12\,\mathrm{Pg\,C\,yr^{-1}}$. These adjustments also reduce the inverted sink in the West region from $0.066 \pm 0.04\,\mathrm{Pg\,C\,yr^{-1}}$ to $0.040 \pm 0.02\,\mathrm{Pg\,C\,yr^{-1}}$ because of high crop consumption and respiration by humans and livestock. The general pattern of sink increase in crop production areas and sink decreases (or source increases) in crop consumption areas highlights the importance of considering the lateral carbon transfer in crop products in atmospheric inverse modeling, which provides an atmospheric perspective of the overall carbon balance of a region.

1 Introduction

Human activities have greatly modified the global carbon cycle through fossil fuel consumption, cement production and land use (Canadell et al., 2007; Le Quéré et al., 2013). The airborne fraction of these carbon sources has been highly variable from year to year mostly due to large variations in the terrestrial carbon sink (Le Quéré et al.,

BGD
11, 6069–6117, 2014

2009). Due to the complexity and heterogeneity of land cover, it has been a challenge to estimate the spatial distribution and the magnitude of terrestrial carbon sources and sinks, and it has been more reliable so far to derive the terrestrial sink as a residual of the global carbon budget than to estimate it using land-based data (Le Quéré et al., 2013). Our ability to project the carbon cycle to the future and its influence on climate will remain limited if we are not able to resolve the current carbon source and sink distribution pattern and provide plausible mechanistic explanations to the pattern. In this regard, regional studies with focuses on the spatial distribution of the carbon cycle would be a useful direction to improve our understanding of the global carbon cycle.

With regard to the carbon cycle, North America may be one of the most closely observed and studied regions in the world. However, the magnitude and the spatial distribution of carbon sinks and sources over the continent are still highly uncertain (Huntzinger et al., 2012; Hayes et al., 2012). In terms of the sink magnitude, atmospheric inversion studies (dubbed "top-down") performed over different time periods from 1992 to 2007 suggest that North America has been a sink ranging from 0.54 to 1.06 $\mathrm{Pg\,C\,yr^{-1}}$ (Gurney et al., 2002, 2003, 2004; Rödenbeck et al., 2003; Baker et al., 2006; Peters et al., 2007; Deng et al., 2013; Peylin et al., 2013), while 19 biospheric models (dubbed "bottom-up") produced an average sink of 0.6 $\mathrm{Pg\,C\,yr^{-1}}$, with a range from −0.7 to 2.2 $\mathrm{Pg\,C\,yr^{-1}}$, for North America over the period from 2000 to 2005 (Huntzinger et al., 2012). Using a biospheric model, Turner et al. (2013) estimated that the net ecosystem productivity (NEP) over North America in 2004 was 1.73 ± 0.37 $\mathrm{Pg\,C\,yr^{-1}}$, and this NEP value is reduced by 0.616 $\mathrm{Pg\,C\,yr^{-1}}$ for the carbon loss due to harvested product emission, river/stream evasion and fire emission in order to estimate the total land sink. These top-down and bottom-up estimates at the continental scale broadly agree, giving us confidence that North America is a large and important contributor to the global terrestrial carbon sink.

In terms of the spatial distribution of the sink within North America, results become more uncertain as the spatial resolution increases. The simple divide of the sink between North American boreal and temperate regions is plagued with uncertainties. For

BGD
11, 6069–6117, 2014

the boreal region, an inversion study (Fan, 1998) produced a sink of $0.2 \pm 0.4\,\mathrm{Pg\,C\,yr^{-1}}$ in 1988–1992, and a TransCom 3 experiment (Gurney et al., 2003) showed a source of $0.26 \pm 0.39\,\mathrm{Pg\,C\,yr^{-1}}$ in 1992–1996. When the TranCom 3 experiment was repeated with updated data, it became a sink of $0.003 \pm 0.28\,\mathrm{Pg\,C\,yr^{-1}}$ in 1992–1996 (Yuen et al., 2005). Using forest inventory data, Canadian forests was found to be a carbon source of $0.069\,\mathrm{Pg\,C\,yr^{-1}}$ in 1985–1989 (Kurz et al., 1999) and Canadian and Alaska forests to be a carbon sink of $0.26 \pm 0.06\,\mathrm{Pg\,C\,yr^{-1}}$ in 1990–2008 (Pan et al., 2011a), while a biospheric model calculated a weak sink of $0.05\,\mathrm{Pg\,C\,yr^{-1}}$ for Canadian forests during 1980s to 1990s (Chen et al., 2003). For the conterminous US with approximately 32 % of the total North America area, estimates of the sink from a set of bottom-up and top-down methods fall in a range from 0.30 to $0.58\,\mathrm{Pg\,C\,yr^{-1}}$ in 1980–1989 (Pacala et al., 2001), while TransCom 3 experiments inferred the sink in 1992–1996 to be 0.89 ± 0.22 and $0.82 \pm 0.40\,\mathrm{Pg\,C\,yr^{-1}}$ for inversions at monthly and annual time steps, respectively (Gurney et al., 2003, 2004; Baker et al., 2006), suggesting that the uncertainty due to the temporal resolution of inverse modeling is considerable. Peters et al. (2007) developed a carbon assimilation system at weekly time steps, named CarbonTracker, and showed that the sink in 2000–2005 in temperate North America is $0.50 \pm 0.60\,\mathrm{Pg\,C\,yr^{-1}}$. With a simple atmospheric budgeting approach applied to CO_2 measurements in the inflows and outflows through the troposphere over conterminous US, Crevoisier et al. (2010) deduced a sink of $0.5 \pm 0.4\,\mathrm{Pg\,C\,yr^{-1}}$ in 2004–2006. Seven other inversion studies, on average, indicate that temperate North America was a sink of $0.685 \pm 0.574\,\mathrm{Pg\,C\,yr^{-1}}$ in 2000–2006 (see summary in Hayes et al., 2012). Although these estimates have large uncertainties, they generally indicate that the major sink in North America is located in the temperate region while the boreal region is either a small sink or source.

The locations of carbon sinks and sources within temperate North America are highly uncertain. The 19 biospheric models employed by Huntzinger et al. (2012) generated very different sink and source spatial patterns over the conterminous USA, although the average sink mostly appears in forested areas in southeast, northeast and north-

BGD
11, 6069–6117, 2014

west regions. Another bottom-up estimate using long-term modeling and recent remote sensing inputs suggested that forests in the southeast region are large sinks because of their predominant mid-age structure (Zhang et al., 2012). Based on forest inventory data, Williams et al. (2012) deduced that forests along the east and west coasts of the USA are large sinks in 2005–2006, with most areas in Arkansas, Louisiana, Mississippi, and Alabama in the southeast region having sinks in the range of 110–140 $g C m^{-2} yr^{-1}$). However, CarbonTracker (Peters et al., 2007) repeatedly produces large sinks in cropland and adjacient grassland areas, while the southeast region varies between a small source to a small sink. Inversion studies that divide North America into 30 regions (11 in the conterminous USA), Deng et al. (2007) and Deng and Chen (2011) indicate broad patterns of the sink distribution in both southeast forest region and mid-west crop region. In these two studies, the seasonal variations of the carbon flux from various terrrestrial ecosystems modeled by a biospheric model and neutralized at the annual time step was used as the prior flux to constrain the inversion. Under the neutralized flux constraint, the inverted sink may be more or less regarded as the atmospheric signal, although the inversion results are inevitably influenced by errors in transport modeling and other prior fluxes such as fossil fuel, biomass burning and ocean-atmospheric exchange. Inversion studies by Peters et al. (2007), Deng and Chen (2011), Lauvaux et al. (2012) and Schuh et al. (2013) indicate that the mid-west croplands persistently behave as a large regional sink, in apparent conflict with our general understanding that croplands do not singificantly accumulate carbon on yearly basis. From the atmospheric perspective, crop production during the growing season results in large uptake of CO_2 from the atmosphere, while crop consumption after harvest takes place in areas outside of croplands. Gourdji et al. (2012) found a large discrepancy between inverse and biospheric model results over crop production and consumption areas in both growing and dormant seasons and attributed this discrepancy to the lack of lateral transfer of agricultural carbon included in biospheric models. Similarly, lateral transfer of carbon also occurs with forest products (Hayes et al., 2012). Hayes et al. (2012) successfully reconciled a large portion of this dis-

BGD
11, 6069–6117, 2014

crepancy using crop and forest product information for North America. Based on this study, it can be inferred that these lateral transports of carbon need to be considered in both bottom-up and top-down modelling in order for them to converge on similar spatial patterns of the carbon sink and source distribution.

In this study, we attempt to improve our top-down modeling methodology through integrating crop production and consumption information in our existing inverse modeling system (Deng and Chen, 2011). The consumption of crop products by livestock and humans is about twice the consumption of forest products (West et al., 2011; Hayes et al., 2012). Unlike forest products with a large range of residence times, crop products can be assumed to be consumed within a year of harvest (West et al., 2011). The spatial distributions of crop production and consumption at the county level (West et al., 2011) provide a sufficient resolution for consideration in atmospheric inverse modeling. The specific objectives of our study are: (1) to investigate the changes in the inverted carbon source and sink distribution after considering the spatial patterns of crop production and consumption, (2) to explore whether these changes improve our understanding of the carbon source and sink distribution within the conterminous USA, and (3) to evaluate the impact of the crop data on the inverted carbon balance for the conterminous USA and other regions of the globe.

2 Atmospheric CO_2 inversion methodology

The Bayesian synthesis inversion method (Enting and Trudinger, 1995) is used in this study. This method includes forward modeling of atmospheric CO_2 concentration using a transport model with prior fluxes and inverse modeling of the surface CO_2 flux based on the difference between modeled and observed CO_2 concentrations.

BGD
11, 6069–6117, 2014

2.1 Forward modeling

2.1.1 Prior fluxes and their uncertainties

The a priori fluxes needed in the Bayesian synthesis inversion include sources from fossil fuel and fire emissions, net carbon exchange between atmosphere and land and between atmosphere and ocean. These fluxes for the time period from 2000 and 2007 used in this study are the same as those used in Deng and Chen (2011) and are summarized in Table 1. The fossil fuel emission field used in this study is constructed based on the fossil fuel CO_2 emission inventory from 1871 to 2006 from the Carbon Dioxide Information Analysis Center (CDIAC) (Marland et al., 2009) and the EDGAR 4 databases on a $1^{\circ} \times 1^{\circ}$ grid (Olivier and Aardenne, 2005). Vegetation fire emissions are a large part of land use changes emissions of up to $2\,\mathrm{Pg\,C\,yr^{-1}}$. The grid point fire emission field used in this research is from the Global Emissions Fire Database version 2 (GFEDv2) (Randerson et al., 2007; van der Werf et al., 2006).

The Boreal Ecosystem Productivity Simulator (BEPS) is employed to produce seasonally varying net ecosystem exchange (NEE) fluxes in hourly time-steps globally (Chen et al., 1999; Ju et al., 2006). Developed based on FOREST Biogeochemical Cycles (FOREST-BGC) (Running and Coughlan, 1988), BEPS was originally intended for modeling the Canadian forest carbon cycle (Chen et al., 2007; Ju et al., 2006; Liu et al., 1999, 2002), but it has been extended to temperate and tropical ecosystems (Higuchi et al., 2005; Matsushita and Tamura, 2002; Sun et al., 2004; Chen et al., 2012). It uses remotely-sensed leaf area index (LAI) (Deng et al., 2006), land cover type from Global Land Cover (GLC2000), meteorology from NCEP-reanalysis (Kalnay et al., 1996), and soil textural data (Webb et al., 1991). A unique feature of BEPS is the separation of sunlit and shaded components in the canopy using not only LAI but also a foliage clumping index (Chen et al., 2005; He et al., 2012) when calculating photosynthesis (Liu et al., 2002; Chen et al., 2012). Given that soil carbon pools are often not well modeled by terrestrial biosphere models, large uncertainties exist in the modeled annual carbon fluxes. However these models are still useful in estimating seasonal and

BGD
11, 6069–6117, 2014

diurnal patterns in response to changes in environmental conditions. Therefore, in most atmospheric inversion studies the prior annual mean NEE from land surfaces at each grid is set to zero (Gurney, 2004; Rödenbeck et al., 2003). The use of seasonally and diurnally varying biospheric fluxes is essential for the forward modeling to include the covariance of atmospheric transport and the surface flux (Denning et al., 1995; Gurney, 2004; Randerson et al., 1997; Deng and Chen, 2011).

In this study, two sets of control terrestrial biosphere fluxes from BEPS are prepared: (1) annually balanced but seasonally and diurnally varying NEE fluxes, and (2) annually, seasonally and diurnally varying NEE fluxes. The annually balanced NEE fluxes are prepared by forcing the annual mean NEE to be zero, resulting in no interannual variability, while the seasonal and diurnal variability is retained. In fulfilling the objectives of this research, cropland carbon adjustments are made to these prior NEE fluxes (see Sect. 3).

The main processes responsible for ocean CO_2 uptake from the atmosphere is the partial pressure difference between the sea surface and the overlying air which in part depends on the seasonal growth of phytoplankton in the oceans. The daily air–sea CO_2 fluxes across the sea surface in this research are simulated by the OPA-PISCES-T model, which is a coupled global circulation model (OPA) (Madec et al., 1998) with an ocean biochemistry model (PISCES-T) (Aumont, 2003; Buitenhuis et al., 2006). This coupled model is forced by daily wind stress, heat and water fluxes from NCEP reanalysis (Kalnay et al., 1996).

The four background surface CO_2 fluxes from 2000 to 2007 are fitted to an hourly $1^\circ \times 1^\circ$ spatial scale as inputs for the forward modeling.

2.1.2 Atmospheric transport

The atmospheric transport model chosen for this research is the transport-only version of the global chemistry Transport Model (Krol et al., 2005), version 5 (TM5), which is an offline model driven by meteorological data from the European Centre for Medium Range Weather Forecast (ECMWF) model. In this study, we define a global grid of $6^\circ \times$

BGD
11, 6069–6117, 2014

4° with nested grids focusing on North America at 3° × 2° based on Peters et al. (2005). The model consists of 25 vertical layers: five layers in the boundary layer, ten in the free troposphere, and ten in the stratosphere. In this study, the prior hourly fluxes are input into TM5 to generate forward simulations of hourly concentrations at 210 CO_2 observation sites over the globe for emissions from fossil fuel consumption ($\boldsymbol{c}_{ff}$), fire ($\boldsymbol{c}_{fire}$), terrestrial biosphere ($\boldsymbol{c}_{bio}$), and oceans ($\boldsymbol{c}_{oce}$).

2.1.3 CO_2 observations

The atmospheric CO_2 concentrations used in this study are the monthly CO_2 observation data from 2000 to 2007 compiled in the GLOBALVIEW-CO_2 2008 database. These concentrations are not actual data but rather baseline conditions which are derived using data integration techniques described by Masarie and Tans (1995). The dataset is compiled with different data types including surface flask, tower, aircraft and ship measurements. In this study, selected months that used measurement-based data from 210 stations are taken to compile the CO_2 concentration matrix, and consist of 12 181 station measurements during the 8 year period from 2000 to 2007. The locations of these stations are shown in Fig. 1.

In order to find the concentration corresponding to the biases in the surface carbon flux to be adjusted through inverse modeling, simulated concentrations corresponding to the prior fluxes need to be subtracted from CO_2 measurements. For continental tower sites, the GLOBALVIEW-CO2 dataset contains weekly averages of measurements in only afternoon hours to capture the well-mixed condition within the planetary boundary layer, and therefore the monthly simulated concentrations at these sites are also taken as average values in the same afternoon hours. For non-tower sites, GLOBALVIEW-CO2 provides a summary of the sample collection times for discrete observations. The simulated concentrations are also sampled at the same times to obtain the monthly mean values, so as to be consistent with the GLOBALVIEW-CO_2 dataset. These monthly averaged simulated concentrations are then subtracted from the corresponding 12 181 monthly CO_2 measurements from GLOBALVIEW-CO2, ex-

BGD
11, 6069–6117, 2014

pressed as follows:

$$\boldsymbol{c} = \boldsymbol{c}_{\text{obs}} - \boldsymbol{c}_{\text{ff}} - \boldsymbol{c}_{\text{fire}} - \boldsymbol{c}_{\text{bio}} - \boldsymbol{c}_{\text{oce}} \quad (1)$$

2.2 Inverse modeling

2.2.1 Inversion regions and concentration locations

The atmospheric CO_2 concentrations are used for inversion of 50 global regions including 30 regions in North America (Fig. 1), following Deng et al. (2007) and Deng and Chen (2011). The 30 regions in North America are delineated based on a 1 km resolution land cover map from AVHRR data (DeFries and Townshend, 1994) and provincial and state boundaries. This nested inversion system allows for a reduction in errors due to spatial aggregation over North America.

2.2.2 Time-dependent Bayesian synthesis approach

We use the time-dependent Bayesian synthesis approach (Enting, 2002) in our inverse modeling. In this approach, a linear combination of source/sink terms is formulated to match with CO_2 concentration observations:

$$\boldsymbol{c} = Gf + A\boldsymbol{c}_0 + \varepsilon, \quad (2)$$

where $\boldsymbol{c}_{m\times 1}$ is a vector of m atmospheric CO_2 observations at given space and times; $\boldsymbol{\varepsilon}_{m\times 1}$ is a random error vector with a zero mean and a covariance matrix $cov(\boldsymbol{\varepsilon}) = \mathbf{R}_{m\times m}$; $\mathbf{G}_{m\times(n-1)}$ is a given matrix representing a transport (observation) operator, where $n-1$ is the number of fluxes to be determined; $\mathbf{A}_{m\times 1}$ is a unity vector (filled with 1) that relates to the assumed initially well-mixed atmospheric CO_2 concentrations ($\boldsymbol{c}_0$); and $f_{(n-1)\times 1}$ is an unknown vector of carbon fluxes of all studied regions. In this research, $m = 12\,181$ (the number of measurements as mentioned in Sect. 2.1.3) and $(n-1) = 4800$ (50 regions × 8 years × 12 months).

BGD
11, 6069–6117, 2014

After combining matrixes **G** and **A** into $\mathbf{M}_{m\times n} = (\mathbf{G}, \mathbf{A})$ and vectors $\boldsymbol{f}$ and $\boldsymbol{c}_0$ as $s_{n\times 1} = (\boldsymbol{f}^T, \boldsymbol{c}_0)^T$, Eq. (2) is rewritten as:

$$\boldsymbol{c} = \mathbf{M}s + \boldsymbol{\varepsilon}. \tag{3}$$

While Eq. (3) can be solved for s by the conventional least-squared technique, the problem is poorly constrained. The Bayes approach (Tarantola, 2005) is generally used for ill-constrained problems through introducing a priori information in the inversion process. The best a priori information for this purpose is a prior estimate of the surface flux. The a posteriori flux is obtained by minimizing the following cost function J:

$$J = \frac{1}{2}(\mathbf{M}s - \boldsymbol{c})^T R^{-1}(\mathbf{M}s - \boldsymbol{c}) + \frac{1}{2}(s - s_\mathrm{p})^T \mathbf{Q}^{-1}(s - s_\mathrm{p}), \tag{4}$$

where $s_{\mathrm{p}_{n\times 1}}$ is the a priori estimate of s (set to zero after subtracting its contribution to concentration from the atmospheric CO_2 observation); the covariance matrix $\mathbf{Q}_{n\times n}$ represents the uncertainty in the a priori estimate; and $R_{m\times m}$ is the model-data mismatch error covariance. Through minimizing this cost function in Eq. (4), the posterior best estimate of s (Enting, 2002) is defined as:

$$\hat{s} = (\mathbf{M}^T R^{-1}\mathbf{M} + \mathbf{Q}^{-1})^{-1}(\mathbf{M}^T R^{-1}\boldsymbol{c} + \mathbf{Q}^{-1}s_\mathrm{p}), \tag{5}$$

with the posterior uncertainty expressed as follows:

$$\hat{\boldsymbol{Q}} = (\mathbf{Q}^{-1} + \mathbf{M}^T R^{-1}\mathbf{M})^{-1}. \tag{6}$$

2.2.3 Transport (observation) operator, model-data mismatch and prior uncertainties

The matrices for transport (observation) operator, **M**, the model-data mismatch, R, and the prior uncertainties, **Q**, are taken from Deng and Chen (2011).

The transport (observation) operator, **M**, is formed from 4800 forward simulations (eight years and 50 regions). An initial flux of 1 Pg C for each month and region was

BGD
11, 6069–6117, 2014

prescribed in the TM5 transport model to find the contribution of each region to CO_2 concentration at each observation site. The model-data mismatch, R, reflects the difference between the modeled and the observed CO_2 concentrations which include both errors from transport modeling and measurement (such as instrument errors). The observation sites were divided into 5 categories, each with its own constant portion (σ_{const}) and variable portion (GVsd) that is computed monthly from the standard deviation data given in GLOBALVIEW-CO2 2008 variation (var) files. The constant portion is defined under the following categories: Antarctic sites (0.15), oceanic sites (0.30), land and tower sites (1.25), mountain sites (0.90), and aircraft samples (0.75). The variable portion is the statistical summary of average atmospheric variability for each measurement record. Therefore, the covariance matrix **R**, is given as a diagonal matrix that contains the error for each month i:

$$\mathbf{R}_{ii} = \sigma^2_{\text{const}} + \text{GVsd}^2. \quad (7)$$

Furthermore, a weighting factor, **W**, is inserted to the cost function in Eq. (4) to account for the vertical correlation between measurements at different levels of the same tower and aircraft sites, i.e. smaller weights are given to each of the measurements at the same site (Deng and Chen, 2011).

$$J = \frac{1}{2}((\mathbf{M}s - \boldsymbol{c})W)^T R^{-1}((\mathbf{M}s - \boldsymbol{c})W) + \frac{1}{2}(s - s_p)^T \mathbf{Q}^{-1}(s - s_p) \quad (8)$$

This weight, W, is a diagonal matrix with the diagonal terms given by:

$$w_{ii} = 1/(1 + 0.6(n - 1)), \quad (9)$$

where n is the number of observations at different levels at the same site.

While the a priori fluxes are set to zero after subtracting their contributions toward the measured CO_2 concentrations, the a priori uncertainties, **Q**, are important in forcing the spatial distribution of the inverted fluxes. These uncertainties are summarized in

BGD
11, 6069–6117, 2014

Table 1. The uncertainties for fossil fuel of ±6 % (Marland et al., 2009) and the fire fluxes of ±20 % (van der Werf et al., 2010) are not included in **Q**, and hence, it is important to note that the inverted fluxes are subject to these additional uncertainties.

The χ^2 test (Gurney et al., 2003) is employed to test the consistency of the fit to CO_2 data and the prior flux estimate simultaneously:

$$\chi^2 = \frac{J_{\min}}{N_{\text{obs}}} = \frac{\sum_{m=1}^{m} \frac{(\mathbf{M}s-\boldsymbol{c})^2}{R^2} + \sum_{n=1}^{n} \frac{(s-s_{\text{p}})^2}{\mathbf{Q}^2}}{N_{\text{obs}}}, \tag{10}$$

where N_{obs} is the number of degrees of freedom (number of observations) and $J_{\min}$ is the cost function from Eq. (4). The consistency of the fit is highest when the value of χ^2 equals unity.

3 US cropland carbon integration methodology

During the growing season, cropland in the US Midwest represents a strong regional carbon sink. However, a large portion of the crops is removed from the location of production during harvest and transported to other regions for storage and consumption. When the crop products are consumed by human and livestock, CO_2 is released back into the atmosphere at geographic locations that differ from the area of crop production. It is important to take into account these patterns, referred to as the lateral transport of cropland carbon, in the prior fluxes used in atmospheric CO_2 inversion studies.

3.1 US cropland carbon budget based on inventory data

The regional patterns of CO_2 uptake and release in US croplands based on agricultural statistics (West et al., 2011) are used to adjust the prior biosphere flux used in our inversion. The datasets can be downloaded from the CDIAC website: http://cdiac.ornl.gov. The data include county-level NPP, harvest, and changes in soil carbon from 1990 to

BGD
11, 6069–6117, 2014

2008, as well as human and livestock crop consumption from 2000 to 2008. The national crop carbon budget for the USA from 2000 to 2008 is balanced within 0.3 to 6.1 % yr^{-1} based on the study from West et al. (2011). Although many other important components are included in the overall US cropland carbon budget, such as exports and crop carbon used for fuel, the vertical net carbon exchange (NCE) into the atmosphere is given by the sum of net carbon uptake from NPP, net change in soil carbon and the release of carbon from biomass decomposition, human consumption and livestock consumption.

3.1.1 Crop NPP, harvest, biomass decomposition and changes in soil carbon pool

The cropland NPP used in West et al. (2011) is calculated based on annual statistics of crop production (P) in units of tons of biomass and harvested crop area (HA) reported by the US Department of Agriculture (USDA), National Agricultural Statistics Service. County level statistics are gap-filled using district level data and then converted to county level NPP in units of carbon using Eq. (11), which is documented in earlier studies (Hicke, 2004; Hicke and Lobell, 2004; Prince et al., 2001; West et al., 2010):

$$\mathrm{NPP}_{\mathrm{crops}} = \sum_i \frac{P_i \times (1 - \mathrm{MC}_i) \times C}{\mathrm{HI}_i \times f_{\mathrm{AG},i} \times \mathrm{HA}_i}, \quad (11)$$

where P is the reported crop production; MC is the harvest moisture content; C is the conversion factor from biomass to carbon (0.45 g of C per g of dry mass); HI is the harvest index, i.e. the ratio of yield mass to above ground biomass; f_{AG} is the fraction of production allocated aboveground; and the subscript i indicates 17 different crops (corn, soybean, oats, barley, wheat, sunflower, hay, sorghum, cotton, rice, peanuts, potatoes, sugarbeets, sugarcane, tobacco, rye and beans) representing the majority of the crops grown in the conterminous US (West et al., 2010, 2011). The harvested

BGD
11, 6069–6117, 2014

amount is calculated based on the crop yields. The carbon released from biomass decomposition is calculated from the NPP by subtracting the amount that is harvested. The remainder of the crops, i.e the amount not harvested, is left as residue and either is sequestered into the soil or decomposes within the same year.

Changes in soil carbon are calculated based on empirical relationships between land management practices and soil carbon change (West et al., 2008). In order to capture the long term impacts on soil carbon pools from a 20 year history of changes in crop rotation and tillage intensity, estimates of soil carbon change were calculated from 1980 to 2008.

3.1.2 Human and livestock consumption

Human crop carbon consumption data provided by West et al. (2011) are calculated based on the per capita food consumption and the US population census data. The livestock consumption data are calculated using a similar method as human consumption but also consider different animal species and their feed consumption rates. The consumed amount is assumed to be released back into the atmosphere within the same year as CO_2 through respiration, excretion and flatus (West et al., 2009). Excretion typically enters the waste treatment facilities within the county and the emissions are taken into account in the consumption term above.

3.2 Prior flux adjustments for US croplands

Integrating carbon exchange due to crop processes into the inversion model requires the NEP modeled by BEPS to be adjusted. For crop processes, the harvested amount is taken away from the field and respired back into the atmosphere when consumed by human, $R_{\text{human\_consumption}}$ and livestock, $R_{\text{livestock\_consumption}}$. Therefore, crop NEP is given by:

$$\text{NEP}_{\text{crop}} = \text{NPP}_{\text{crop}} - R_{\text{h, residue}} - R_{\text{human\_consumption}} - R_{\text{livestock\_consumption}} + \Delta \boldsymbol{c}_{\text{soil}} \quad (12)$$

BGD
11, 6069–6117, 2014

Since the residue amount, including both the remaining aboveground and belowground biomass, is the difference between the total crop biomass and the amount harvested, Eq. (12) can be rewritten as:

$$\begin{aligned} NEP_{crop} &= NPP_{harvested} + \Delta c_{soil} - R_{human\_consumption} - R_{livestock\_consumption} \\ &= \text{production-consumption} \end{aligned} \quad (13)$$

where,

$$\text{production} = NPP_{harvested} + \Delta c_{soil} \quad (14)$$

$$\text{consumption} = R_{human\_consumption} + R_{livestock\_consumption} \quad (15)$$

The spatial patterns of the crop production, consumption and NEP are shown in Fig. 2. The spatial distributions of crop production and consumption are calculated monthly and are used to adjust the monthly NEP distributions modeled by BEPS over the conterminous USA. The production and the consumption terms are adjusted separately due to their different seasonal patterns.

3.2.1 Production adjustment

The simulated terrestrial NPP by BEPS is adjusted to integrate cropland production over the contiguous US using the equation below:

$$\begin{aligned} NPP_{adjusted} &= NPP_{biosphere} - r_{crop\_area} \cdot (NPP_{biosphere}) + \text{production} \\ &= (1 - r_{crop\_area}) \cdot NPP_{biosphere} + \text{production} \\ &= (1 - r_{crop\_area}) \cdot NPP_{biosphere} + NPP_{harvested} + \Delta c_{soil}, \end{aligned} \quad (16)$$

where $NPP_{biosphere}$ is the $1^\circ \times 1^\circ$ NPP output from BEPS and r_{crop_area} is the ratio of harvested crop area within the $1^\circ \times 1^\circ$ grid over the total area of the grid. The county-level cropland production is first extrapolated into a mean value for each $1^\circ \times 1^\circ$ grid,

BGD
11, 6069–6117, 2014

then adjusted using Eq. (16). The ratio $r_{\text{crop\_area}}$ is calculated based on the harvested area data. The basic idea of Eq. (16) is to replace BEPS NPP with more accurate crop production data. BEPS uses GLC2000 as the land cover data in NPP simulations, but these data are not as accurate as the agricultural statistics in terms of the crop area within each grid. Chan and Lin (2011) cautioned researchers against the direct comparison of carbon accounting based on agricultural census data and TBM simulated fluxes due to large differences of different land cover classifications used. For this reason, we choose to use the crop area ratio method for the production adjustment.

Since the prior surface CO_2 fluxes enter into the atmospheric transport model on hourly time steps, the annual crop carbon production data are interpolated into the seasonal and diurnal patterns simulated in the BEPS model. Firstly, the annual $\text{NPP}_{\text{biosphere}}$ is converted to annual $\text{NPP}_{\text{adjusted}}$, then the ratio between the two is taken and multiplied by the hourly $\text{NPP}_{\text{biosphere}}$ fluxes, resulting in hourly adjusted fluxes from 2000 to 2008 for each $1^\circ \times 1^\circ$ grid.

3.2.2 Consumption adjustment

The consumption terms are integrated into BEPS-simulated R_h over the contiguous US using the following equation:

$$\begin{aligned} R_{\text{h, adjusted}} &= R_{\text{h, biosphere}} - r_{\text{crop\_area}} \cdot (R_{\text{h, biosphere}}) + \text{consumption} \\ &= (1 - r_{\text{crop\_area}}) \cdot R_{\text{h, biosphere}} + \text{consumption} \\ &= (1 - r_{\text{crop\_area}}) \cdot R_{\text{h, biosphere}} + R_{\text{human\_consumption}} + R_{\text{livestock\_consumption}} \end{aligned} \quad (17)$$

where $R_{\text{h, biosphere}}$ is the $1^\circ \times 1^\circ R_h$ output from BEPS and $r_{\text{crop\_area}}$ is the ratio of harvested crop area within the $1^\circ \times 1^\circ$ grid over the total area of the grid. The county-level cropland consumption data are first resampled into each $1^\circ \times 1^\circ$ grid, and the mean value of each grid is used to adjust R_h using Eq. (17). However, unlike the production adjustment, the temporal patterns of CO_2 release from human and livestock consumptions do not follow the seasonal and diurnal patterns simulated for the biosphere. We

BGD
11, 6069–6117, 2014

therefore assume constant hourly release of CO_2 from crop consumption throughout the year. In this way, the annual consumption amount is divided equally into the hourly values and added to the hourly simulated $R_{h,\ biosphere}$ from BEPS for the time period from 2000 to 2008 at each 1° × 1° grid.

3.3 Schemes of inversion experiments

Two sets of experiments outlined in Table 2 are designed to test for the impact of integrating the cropland carbon data into the prior terrestrial flux. In the first set (Experiments 1a, 1b, 1c), the monthly terrestrial biosphere NEP modeled by BEPS at hourly time steps is first neutralized on the annual basis, meaning that the annual mean terrestrial flux is 0 for each grid cell but its seasonal variation is retained. This neutralized flux is then adjusted for crop production and consumption in Experiments 1b and 1c. The prior terrestrial surface flux in many atmospheric inversion studies only contains seasonal instead of interannual variations (Gurney, 2004; Rödenbeck et al., 2003) in order to minimize the influence of the errors in the prior flux on the inverted annual flux so that the results are based on the "atmospheric view". In the second set (Experiments 2a, 2b, 2c), the same monthly BEPS NEP is used without annual neutralization so that both seasonal and interannual variations in NEP are retained and the best estimate of the biospheric carbon flux is used to constrain the inversion. Experiments 1a–c are therefore designed to explore the strength of the carbon cycle signal in the atmospheric CO_2 measurement, while Experiments 2a–c are considered to be the best final estimates by integrating ecosystem modeling results and crop statistics. In each set of experiments, there is a control run (Experiments 1a, 2a), based on which the influences of the production adjustment (Experiments 1b, 2b) and the production and consumption adjustments (Experiments 1c, 2c) on the inverted flux are assessed.

The a priori uncertainty matrix **Q** described in Sect. 2.2.3 is adjusted to take into account the uncertainties from the cropland production and consumption data. Uncertainties in the agricultural production data include the large uncertainties in the parameters used, including the harvest index (HI) and reported crop production (P) (Chan

BGD
11, 6069–6117, 2014

and Lin, 2011). Bolinder et al. (2007) and Prince et al. (2001) show the standard deviation of HI, the dominant source of uncertainty towards NPP, to be 10 %. Therefore, experiments that adjust for the production only are prescribed a 10 % uncertainty in the annual NPP found in the agricultural statistics data distributed over the production regions and weighted with the original matrix **Q**. Experiments that adjust for both the production and the consumption use the above method to include the production uncertainty as well as an additional 1 % of annual total human consumption (West et al., 2009) and 20 % of the annual total livestock consumption distributed over consumption areas (Ciais et al., 2007). Furthermore, the χ^2 test (Eq. 12) is employed to show the consistency of the fit to data and prior flux estimates simultaneously. The χ^2 values are also shown in Table 2, indicating that Experiments 1c and 2c with the χ^2 values closest to unity have the highest consistency.

4 Results and discussion

The inversion experiments described in Sect. 3.3 are conducted to test the impacts of cropland inventory on the inverted CO_2 fluxes. The impacts are evaluated based on the multi-year mean annual values and seasonal variations.

4.1 Multi-year regional carbon budget

4.1.1 Average annual flux

The average annual inverted CO_2 fluxes over the conterminous USA are shown for Experiment 1 and Experiment 2 in Figs. 3 and 4, respectively. Table 3 summarizes the mean inverted CO_2 fluxes (μ) and errors (ε), as well as percentage changes (Δ %) from the control case calculated by:

$$\Delta\,\% = \frac{\mu - \mu_{\text{control}}}{\mu_{\text{control}}}, \tag{18}$$

BGD
11, 6069–6117, 2014

where $\mu_{control}$ is the annual mean inverted flux for the control experiment.

To evaluate the impact of integrating crop production and consumption data into the prior fluxes, comparisons of the inverted fluxes can be made between the experiments with and without crop adjustments. However, in order for these comparisons to be meaningful, a signal-to-noise ratio (SNR) is calculated for each region, using the following equation:

$$\mathrm{SNR} = \frac{|\mu - \mu_{control}|}{\varepsilon}. \quad (19)$$

where ε is the posterior uncertainty in the inverted flux for a region. Note that the "signal" here is defined as the mean difference in the inverted fluxes between the control and a crop-adjusted experiment, in order to represent the signal introduced by the adjustment. If SNR is less than unity, the resulting change due to an agricultural adjustment is less than the uncertainty, and hence the signal is within the noise level of the results. In Table 3, regions with SNR greater than unity is denote with "*".

Comparing Fig. 3a and b, it can be seen that the production adjustment redistributed the carbon sink from forested regions in the Southeast (Regions 26 to 28) and Northwest (Regions 18, 19) to cropland area in the Midwest (Regions 20 and 21). SNR for the Experiment 1b for Region 20 is greater than 1 (Table 3), indicating that the sink increase there is beyond inversion uncertainty. The increase in the sink size in the US Midwest can be attributed to the large CO_2 uptake during the growing season, but much of the carbon is released through crop consumption in other geographic locations. Seasonal results for these regions are shown in Session 4.3.

The impact of crop consumption adjustment on the inversion result can be assessed by comparing Fig. 3b and c. In Region 28 with large crop consumption, the inverted carbon sink (Fig. 3c) is reduced by 36 % from the case with crop production adjustment only (Fig. 3b) and by 54 % from the control case (Fig. 3a), which is a sink $-69\,\mathrm{Tg\,C\,yr^{-1}}$ (Table 3). In Regions 23 and 24 with large crop consumption and low vegetation growth, the crop consumption adjustment turns weak carbon sinks (Fig. 3a and b) into sources

BGD
11, 6069–6117, 2014

(Fig. 3c). SNR for Experiment 1c for Region 24 (California) is greater than 1, confirming that this shift from sink to source is beyond the inversion uncertainty. In general, crop consumption adjustment in regions with considerable consumptions (Regions 18, 19, 23, 24, 25, 26, 27, 28) induces noticeable reduction in the carbon sink. It would also be interesting to note that the crop production adjustment (Experiment 1b) increases the USA sink by 17 % but decreases the Canadian sink by 13 %, and the crop production and consumption adjustments (Experiment 1c) reduces the sink by 0.8 % and 8.4 % for USA and Canada, respectively, relative to the control case (Experiment 1a, Table 3). These results suggest that the crop information used in the inversion not only affects USA carbon sinks but also neighboring regions (such as Canada). The inverted results from both crop production and consumption adjustments (Experiment 1c, Fig. 3c) show that the US Midwest sink in 2002–2007 is $0.363 \pm 0.13\,\mathrm{Pg\,C\,yr^{-1}}$. This sink value obtained in Experiment 1c is similar to that ($263\,\mathrm{Pg\,C\,yr^{-1}}$) in Experiment 1b but considerably larger than $189\,\mathrm{Pg\,C\,yr^{-1}}$ in the control case, confirming the importance of considering the crop production and consumption data for atmospheric inversion.

Experiments 1a–c analyzed above are designed to accentuate the information content of atmospheric CO_2 measurements for the surface carbon flux by neutralizing the annual biospheric fluxes before making the crop consumption adjustments. However, it could be argued that the annually neutralized fluxes may not be the best prior information for constraining the inversion. Experiments 2a–c are therefore conducted with the best prior estimates possible based on a biospheric model and crop data. The prior biospheric carbon flux used in Experiment 2 differs from that in Experiment 1 in the following ways: (1) the annual net carbon flux modeled by BEPS is used without neutralization, (2) the interannual variations in the prior flux are considered, and (3) the interannual variations in crop production and consumption are also considered. Although errors in the annual mean prior fluxes would have imprints on the inverted results in Experiment 2, the un-neutralized fluxes may nudge the inverted results closer to the reality as it integrates our prior knowledge on the carbon source and sink distribution and the interannual variability.

BGD
11, 6069–6117, 2014

Figure 4 shows inverted results under Experiment 2 with comparisons to the prior estimates in three cases: Experiment 2a with the biospheric flux from BEPS only, Experiment 2b with the biospheric flux adjusted by crop production, and Experiment 3c with the biospheric flux adjusted by both crop production and consumption. The production adjustment (Experiment 2b) leads to significant increases in the CO_2 sink in the Midwest crop area (Regions 20). Regions 19, 21 and 25 also gain noticeable sink increases, but sinks in other regions in USA decrease in compensation for these gains. Relative to Experiment 2b, the additional consumption adjustment made in Experiment 2c significantly weakened the sinks in the West region and noticeably in the Southeast. These results are consistent with the findings from Experiment 1. Crop adjustments in Experiment 2 greatly enhanced the sinks in the cropland in the US Midwest (Regions 20, 21), mostly at the expense of forested areas in the Southeast (Regions 26, 27, 28). This is also similar to Experiment 1, which only takes into account the seasonal variations but not the interannual variations. For the purpose of comprehensive evaluation of how crop adjustments spatially redistribute the carbon flux, Table 4 provides a matrix of correlation coefficients of the change in the inverted flux from Experiment 2a to Experiment 2c among the 11 regions in the USA, where positive (negative) correlations indicate that the crop adjustments make the inverted flux to increase or decrease in the same (opposite) direction. Region 21, for example, is negatively correlated with most regions except Regions 20, 23 and 24, suggesting that its increase in carbon sink after the crop adjustments is mostly balanced by decreases in other regions except Regions 20, 23, and 24.

Our Experimental 2a result for Region 20 is comparable to the sink of $0.11\,\mathrm{Pg\,C\,yr^{-1}}$ for cropland in about the same region from 2001 to 2005 reported by Peters et al. (2007), in which the biospheric flux was not adjusted for crop production and consumption. After crop adjustments in Experiment 2c, the sink magnitude in Region 20 is about doubled with a total of $0.23\,\mathrm{Pg\,C\,yr^{-1}}$ (Table 3) or $298\,\mathrm{g\,C\,m^{-2}\,yr^{-1}}$. The corresponding sink magnitude in Region 21 is $0.19\,\mathrm{Pg\,C\,yr^{-1}}$ or $181\,\mathrm{g\,C\,m^{-2}\,yr^{-1}}$. The average sink strength of these two region ($219\,\mathrm{g\,C\,m^{-2}\,yr^{-1}}$) is about 45 % larger than

BGD
11, 6069–6117, 2014

the results (about 150 g C m^{-2} yr^{-1}) of three inversion models used in the Mid-Continent Intensive (MCI) study (Schuh et al., 2013). The MCI study area of 1000 km × 1000 km covers 52 % of Regions 20 and 21, and the total inverted sink was about 0.15 Pg C yr^{-1}. In another inversion study (Lauvaux et al., 2012), the inverted sink for the same MCI area was 0.183 Pg C over a growing season from June to December (the dormant season was about carbon neutral). The inverted sink per unit land area over a corn grid was found to be about 50 % smaller than eddy covariance flux measurements at the same location, although a mixture of crop and grassland in the grid is given as the probable reason for this large discrepancy. The difference of our inversion results from these MCI studies is within the posterior uncertainty of our inversion but also indicates the need of further evaluation of our inversion results.

Table 3 also provides aggregated results for 4 large USA census regions: West, Midwest, Northeast and Southeast, as well as for USA and Canada. Crop consumption adjustments make significant (SNR > 1) changes to the inverted carbon flux in the West region in both Experiments 1 and 2. This is mostly due to the large crop consumption in California. In Experiment 2b with the non-neutralized and interannually variable prior biospheric flux, the crop production adjustment alone affects very little the inverted sink in the West region, but significantly increases the sink in the Midwest region with high crop production. Similar to Experiment 1, the total sinks in North America and Canada show large changes in sink sizes for Experiment 2 after crop adjustments. This suggests that in atmospheric inversion, the changes in the a priori flux affect the inverted results not only locally but also globally (Gurney, 2004). The overall USA and North American carbon sinks are both shown to have increased when adjusted for production only in Experiment 2b, whereas their sink sizes are similar to the control case when the crop consumption adjustment is also made (Experiment 2c), where the percentage changes are only 1.7 % and −2.6 % (Table 3), respectively. This result reinforces our original assumption that the long term cropland carbon budget is approximately balanced between the crop production and consumption (West et al., 2011).

BGD
11, 6069–6117, 2014

4.2 Multi-year global carbon budget

Although the cropland carbon adjustments were only made for the US regions, the CO_2 flux is inverted globally. Table 5 provides the average annual inverted CO_2 fluxes globally from 2002 to 2007 for Experiments 1 and 2. It also summarizes the mean inverted CO_2 fluxes (μ) and errors (ε), as well as percentage changes (Δ %) from the control case for the large regions outside of North America. In the results for both Experiments 1 and 2, changes in the inverted flux are observed in many regions outside of the USA, although no adjustments to the prior flux were made outside of USA. A plausible explanation for these results is that any changes in the total sinks in the conterminous USA must be compensated by other regions around the globe since the global carbon budget is constrained by the mean changes in the atmospheric CO_2 concentration. In an atmospheric inversion study, Gurney (2004) found that contributions from land fluxes appeared in the adjacent ocean regions, and described this phenomenon as flux "leakage". In our case, the compensating effect seen in other regions outside of the conterminous USA may also be considered as a leakage. This leakage puts into question the reliability of the atmospheric CO_2 measurements in optimizing the local flux if the prior information is biased, given the fact that North America is one of the continents with strong data constraints.

The inverted total global land sink from Experiment 2 is larger than that from Experiment 1 (Table 5) because the prior land sink in Experiment 2 is larger than that in Experiment 1. To compensate this influence of the prior flux over land, the inverted ocean sink is smaller in Experiment 2 than in Experiment 1. The total land and ocean sinks do not show large changes with the crop production or crop consumption adjustments in the USA in both experiments (Table 5). Relative to Experiment 1, Experiment 2 shows a slightly larger decrease in the terrestrial sink and a slightly larger increase the ocean sink. The overall crop adjustments allocate a slightly smaller sink to North America while most regions outside of North America adjust accordingly to balance the global carbon budget due to weak data constraints in other regions.

BGD
11, 6069–6117, 2014

4.2.1 Seasonal variation

The timings of the CO_2 uptake and release from croplands exert great influences on the atmospheric CO_2 (Corbin et al., 2010), as crops in different regions differ in their growth patterns. The seasonal variation pattern in the surface flux may coincide with that in the strength of atmospheric boundary layer mixing, causing the rectifier effect on atmospheric transport (Denning et al., 1995; Gurney, 2004). In this research, the a priori seasonal variation for cropland is based on BEPS which considers the seasonal variations in vegetation structure using remotely sensed LAI and meteorology. Figure 5 shows the monthly a priori and a posteriori CO_2 fluxes for the period of 2002–2007 from Experiment 2 for regions of high crop production and high crop consumption in the US. Results from Experiment 1 are not shown, but they are similar in the seasonal variation pattern.

In Regions 20 and 21 of high crop production, the inverted monthly fluxes with agricultural adjustments show higher uptake during the peak growing season of June, July and August and a stronger release of carbon during the non-growing season in October and November than the prior fluxes. March and April show a net uptake in the CO_2 inverted fluxes in agriculturally adjusted experiments in Region 20 instead of near carbon neutrality shown in the control experiment. In Regions 23 and 24 of high crop consumption with low vegetation, the impacts of crop consumption adjustment are mostly shown as persistent decreases in sinks throughout the year, while those of the production adjustment as persistent increases. In the forests in the US Southeast with moderate crop production and consumption (Regions 26, 27, 28), the crop production adjustment (Experiment 2b) and the crop production and consumption adjustments (Experiment 2c) have discernible to considerable impacts on the magnitude of the CO_2 uptake during the growing season and release during non-growing seasons.

The changes in the monthly inverted fluxes after adjusting for crop production and consumption are mainly observed as changes in the magnitude instead of the timing of the growing seasons. This means that the seasonal pattern of the inverted CO_2

BGD
11, 6069–6117, 2014

flux generally follows that of the a priori flux. In making our US cropland carbon adjustments, annual cropland census data are used instead of actual cropland seasonal variations, while the seasonal growth pattern is modeled based on remotely sensed LAI and meteorology. Therefore, these results are constrained by remote sensing information, although they are also subject to certain uncertainties due to errors in retrieved LAI and the model.

4.3 Discussion

After integrating US crop production and consumption data into the prior flux, the US Midwest becomes a large regional CO_2 sink from 2002 to 2007 in our inverse modeling. This is mainly due to the large uptake of CO_2 during the growing season (Peters et al., 2007). Because of the release of the CO_2 in regions of sizable crop consumptions by humans and livestock, a weakening of the US Southeast forest sink is found in our inversion. With the neutralization of the annual prior flux before adjusting for crop consumption (Experiment 1), the US Midwest is perceived by the "atmospheric view" as the dominant sink in North America. While croplands in the US Midwest uptake large amounts of carbon during the growing season, some of this carbon is decomposed onsite while the remainder is transported offsite and respired back to the atmosphere elsewhere. Therefore, lateral transport of carbon needs to be considered in order to reconcile atmospheric inversion results with ground-based measurements (Hayes et al., 2012; Gourdji et al., 2012). In the West Coast including California, where there are high human and livestock consumptions, an overall CO_2 source is obtained from the inversion. With the incorporation of US cropland carbon data, the main US sink is redistributed from the US Southeast and West forested regions to the US Midwest cropland in the inversion process. In order to assess the possible range of errors in our inversion system, this redistribution is shown in the results from two sets of experiments. Experiment 1, which gives larger weights to the influence of atmospheric CO_2 observation than to the prior terrestrial flux, shows the sink in the US Midwest to be larger than that in the US Southeast. Similar results are also obtained in Experiment 2, which gives

BGD
11, 6069–6117, 2014

larger weights to the prior terrestrial flux as an opposite case. In both experiments, the inclusion of agricultural inventory data in the priors significantly altered the inversion results for several regions in the West and Midwest regions.

In Experiment 1 based on an annually neutralized prior ecosystem flux, the overall magnitudes of the US and North American sinks are weakened by ~ 0.8 % and ~ 4.4 % after the cropland production and consumption adjustments are made. Furthermore, regions outside of the USA are also affected by these adjustments, and the Canadian carbon sink shows noticeable weakening (8.4 %). Many regions outside of North America, which are not as well constrained by CO_2 observations, also show small changes when these adjustments are made. While these changes may have been affected by the additional errors introduced to the uncertainty matrix of the prior flux to consider errors in these adjustments, the leakage of the CO_2 flux from the adjusted regions into other regions with poor constraints may be the main reason for these changes (Gurney, 2004). While not conclusive, this phenomenon of leakage points to the importance of the prior flux for constraining atmospheric inversion for the carbon flux of small regions with sparse atmospheric CO_2 measurements. It is also interesting to note that in Experiment 2, which uses an un-neutralized prior flux, this leakage phenomenon is greatly reduced, presumably due to the fact that the un-neutralized flux is closer to reality than the neutralized flux. The following further discussion is therefore based on results from Experiment 2.

During the period from 2002 to 2007, the annual mean crop production and consumption over the conterminous USA based on West et al. (2011) were ~ $0.27\,\mathrm{Pg\,C\,yr^{-1}}$ and ~ $0.24\,\mathrm{Pg\,C\,yr^{-1}}$, respectively. The consumption is smaller than production by about $0.03\,\mathrm{Pg\,C\,yr^{-1}}$, which is close to the value of $0.047\,\mathrm{Pg\,C\,yr^{-1}}$ for US agricultural carbon export in 2008 estimated by West et al. (2011). For the US Midwest, the inverted results with agricultural adjustments show a large sink of $0.42 \pm 0.13\,\mathrm{Pg\,C\,yr^{-1}}$ (Experiment 2c). The value is reduced to $0.24\,\mathrm{Pg\,C\,yr^{-1}}$ if these adjustments are not made (Experiment 2a). These adjustments make a difference of approximately 67 % of the total annual crop production in the USA (West et al., 2011).

BGD
11, 6069–6117, 2014

This suggests that the NEP simulations from the Boreal Ecosystem Productivity Simulator (BEPS) underestimate the processes that relate to cropland CO_2 sinks because it assumes the consumption (respiration) occurs at the same location as production.

The US West and Southeast, being regions of large population and crop consumption, show a combined 0.145 $PgC\,yr^{-1}$ weakening of the sink after the crop adjustments (Experiment 2c). This sink reduction is about 60 % of the total annual crop consumption averaged over 2002 to 2007 ($\sim 0.24\,PgC\,yr^{-1}$, based on West et al. (2011)), indicating the importance of using the crop consumption data for these two regions in the inversion.

Using an atmospheric inversion technique over North America, Peters et al. (2007) showed the US Midwest to be the major sink and the US Southeast forest region to be either carbon neutral or a source between 2002–2007. In our inversion constrained by the annually neutralized a priori flux adjusted for crop production and consumption (Experiment 1c, Table 3), the US Midwest is also shown to be a large CO_2 sink, but the US Southeast forest region remains a sizable carbon sink of $0.158 \pm 0.12\,PgC\,yr^{-1}$ in the same period. Our result differs from that of Peters et al. (2007) for the US Southeast mostly because of different prior fluxes used. Our inversion with the un-neutralized prior flux modeled by BEPS (Experiment 2a) produced a large sink of $0.413 \pm 0.115\,PgC\,yr^{-1}$ for the Southeast (Table 3), and with crop production and consumption adjustments to the un-neutralized prior flux (Experiment 2c), the Southeast still remains a strong sink of $0.29 \pm 0.12\,PgC\,yr^{-1}$. From the neutralized experiments, we can infer that the atmospheric signal is forcing the inversion in the sink direction for the US Southeast. Although the sink is reduced by 42 % when crop production and consumption in this region are considered, this atmospheric signal seems to be robust in indicating this region to be a large sink. The results from Experiment 2 show that this sink signal is considerably strengthened if the prior flux is a sink, as we would expect from bottom-up modeling (Zhang et al., 2012) for forests considering the predominant mid-age forest structure (Pan et al., 2011b). The results of crop consumption adjustment obtained

BGD
11, 6069–6117, 2014

in Experiments 1c and 2c give us confidence that the crop consumption in the US Southeast is not large enough to offset the forest sink in this region.

The main components of the US cropland carbon budget presented by West et al. (2011) are the crop production and consumption. However, there is also a significant portion of the crop products being exported outside of the USA. Ciais et al. (2007) shows the importance of this lateral transport of carbon internationally. In our study, this lateral international transport of crop carbon is not considered, but its effects on the US carbon cycle might have been included to the first order by the difference between crop production of $\sim 0.27\,\mathrm{Pg\,C\,yr^{-1}}$ and crop consumption of $\sim 0.24\,\mathrm{Pg\,C\,yr^{-1}}$ within USA.

While the use of census-based cropland carbon data is cautioned due to their potentially large uncertainties (Chan and Lin, 2011), our research shows that agricultural statistical data give valuable information on the spatial patterns and the magnitude of the surface CO_2 flux. Cropland carbon and atmospheric CO_2 data, when used in combination, are shown to be able to optimize the prior terrestrial CO_2 flux simulated by a biospheric model and can suggest areas of improvement in the model. This research shows that for managed land cover types such as croplands, where the carbon uptake and release are not simply determined by biospheric processes, biospheric models should not be the only tool used for generating prior terrestrial surface CO_2 fluxes (Ciais et al., 2007). Inventory data, such as agricultural statistics, are shown in this research to provide the missing spatial information useful for regional carbon budget estimation using atmospheric inversion techniques.

5 Conclusion

Through adjusting the prior terrestrial carbon flux from a biospheric model using crop production and consumption data at the county level over the conterminous USA, we conducted two sets of atmospheric inversion experiments for the purpose of investigating the influence of the crop data on the spatial distribution of the inverted carbon flux over North America from 2002 to 2007. One set of experiments utilizes the prior

BGD
11, 6069–6117, 2014

flux that is annually neutralized before the adjustments, and the other set utilizes the prior flux without the neutralization. These two sets of experiments allow us to explore the possible ranges of the influences of the crop data on the inverted carbon flux. The main findings of this research are summarized as follows:

1. The spatial distribution of the inverted carbon flux among 30 regions in North America is sensitive to changes in the prior flux after the crop production and consumption adjustments. An atmospheric sink signal is detected in cropland areas because of crop production, while a source signal is detected elsewhere due to crop consumption. Similar to many other biopheric models, the model used in this study provides a prior carbon flux without considering the lateral transport of carbon and therefore does not capture the large consumption sources and underestimates the large production sinks. While we agree with Gurney et al. (2003) who suggested that inverted fluxes are insensitive to small changes in the a priori fluxes for regions well constrained by atmospheric data, our results show that lateral carbon transport adjustments to the a priori flux are large enough to significantly alter the spatial distribution of the inverted flux. In some crop production and consumption regions, changes in the inverted flux are larger than the uncertainty estimate. Although West et al. (2011) shows the annual cropland carbon budget to be approximately balanced over conterminous US, the spatial distributions of crop production and consumption are highly uneven, and it would be useful to integrate this information into the prior flux in atmospheric inversion systems. We therefore agree with the suggestion of Ciais et al. (2007) that simply forcing the prior fluxes in inversions to follow spatial patterns of NPP is not compatible with regional patterns of CO_2 sources and sinks due to crop product displacement.

2. Integration of crop data in the prior fluxes has helped identify some robust atmospheric signals in some source and sink regions. Similar to Peters et al. (2007), we also find the US Midwest to be a large CO_2 sink due to crop production, whether or not the production and consumption adjustments are made or the prior flux

BGD
11, 6069–6117, 2014

is neutralized. Dissimilar to Peters et al. (2007), we find the forest regions in the US Southeast to be a considerable sink. The neutralization of the prior flux and the adjustments for crop consumption make the sink smaller, but these regions remain sizable sinks throughout the inversion period from 2002 to 2007. This robust signal confirms the finding of Zhang et al. (2012) that the US Southeast is a large sink because of the large fraction of mid-age, actively growing forests. The usage of the crop data has helped reconcile top-down and bottom-up results, in agreement with Hayes et al. (2012).

3. The crop adjustments made to the prior carbon flux over the conterminous USA also noticeably altered the inverted flux outside the USA when the biospheric flux is neutralized on an annual basis. This seems to be a leakage of the flux to regions outside of the adjusted regions, a similar case to that was previously found by Gurney (2004). Without sufficient atmospheric CO_2 data to constrain each region, the alteration of the flux in one region is mostly compensated by other regions, especially those in vicinity and least constrained. This result confirms that our current ground-based CO_2 observation network is not dense enough in any region in the world to conduct inversions without the additional prior flux constraint. Therefore, more attention should be given to obtaining accurate prior fluxes for inversion purposes or greatly expanding the current CO_2 observation network.

Acknowledgements. This research is supported by a research grant (2010CB950704) under the Global Change Program of the Chinese Ministry of Science and Technology, an individual grant (GR-646) from the previous Canadian Foundation of Climate and Atmospheric Sciences (CFCAS), and a Canada Research Chair program.

References

Aumont, O.: An ecosystem model of the global ocean including Fe, Si, P colimitations, Global Biogeochem. Cy., 17, 1060, doi:10.1029/2001GB001745, 2003.

BGD
11, 6069–6117, 2014

Baker, D., Law, R. M., Gurney, K. R., Rayner, P. J., Peylin, P., Denning, A. S., Bousquet, P. Bruhwiler, L., Chen, Y.-H., Ciais, P., Fung, I. Y., Heimann, M., John, J., Maki, T., Maksyutov, S., Masarie, K., Prather, M., Pak, B., Taguchi, S., and Zhu, Z.: TransCom 3 inversion intercomparison: impact of transport model errors on the interannual variability of regional CO_2 fluxes, 1988–2003, Global Biogeochem. Cy., 20, 1988–2003, doi:10.1029/2004GB002439, 2006.

Bolinder, M. A., Janzen, H. H., Gregorich, E. G., Angers, D. A., and VandenBygaart, A. J.: An approach for estimating net primary productivity and annual carbon inputs to soil for common agricultural crops in Canada, Agr. Ecosyst. Environ., 118, 29–42, doi:10.1016/j.agee.2006.05.013, 2007.

Buitenhuis, E. T., Le Quéré, C., Aumont, O., Beaugrand, G., Bunker, A., Hirst, A., Ikeda, T., O'Brien, T., Piontkovski, S., and Straile, D.: Biogeochemical fluxes through mesozooplankton, Global Biogeochem. Cy., 20, 1–18, doi:10.1029/2005GB002511, 2006.

Canadell, J. G., Le Quéré, C., Raupach, M. R., Field, C. B., Buitenhuis, E. T., Ciais, P., Conway, T. J., Gillett, N. P., Houghton, R. A., and Marland G.: Contributions to accelerating atmospheric CO_2 growth from economic activity, carbon intensity, and efficiency of natural sinks, P. Natl. Acad. Sci. USA, 104, 18866–18870, doi:10.1073/pnas.0702737104, 2007.

Chan, E. C. and Lin, J. C.: What is the value of agricultural census data in carbon cycle studies?, J. Geophys. Res., 116, 1–14, doi:10.1029/2010JG001617, 2011.

Chen, B., Chen, J. M., Mo, G., Yuen, C.-W., Margolis, H., Higuchi, K., and Chan, D.: Modeling and scaling coupled energy, water, and carbon fluxes based on remote sensing: an application to Canada's landmass, J. Hydrometeorol., 8, 123–143, doi:10.1175/JHM566.1, 2007.

Chen, J. M., Liu, J., and Cihlar, J.: Daily canopy photosynthesis model through temporal and spatial scaling for remote sensing applications, Ecol. Model., 124, 99–119, doi:10.1016/S0304-3800(99)00156-8, 1999.

Chen, J. M., Ju, W., Cihlar, J., Price, D., Liu, J., Chen, W., Pan, J., Black, T. A., and Barr, A.: Spatial distribution of carbon sources and sinks in Canada's forests, Tellus B, 55, 622–641, 2003.

Chen, J. M., Menges, C. H., and Leblanc, S. G.: Global derivation of the vegetation clumping index from multi-angular satellite data, Remote Sens. Environ., 97, 447–457, 2005.

Chen, J. M., Mo, G., Pisek, J., Deng, F., Ishozawa, M., and Chan, D.: Effects of foliage clumping on global terrestrial gross primary productivity, Global Biogeochem. Cy., 26, GB1019, doi:10.1029/2010GB003996, 2012.

BGD
11, 6069–6117, 2014

Ciais, P., Bousquet, P., Freibauer, A., and Naegler, T.: Horizontal displacement of carbon associated with agriculture and its impacts on atmospheric CO_2, Global Biogeochem. Cy., 21, 1–12, doi:10.1029/2006GB002741, 2007.

Corbin, K. D., Denning, A. S., Lokupitiya, E. Y., Schuh, A. E., Miles, N. L., Davis, K. J., Richardson, S. and Baker, I. T.: Assessing the impact of crops on regional CO_2 fluxes and atmospheric concentrations, Tellus B, 62, 521–532, doi:10.1111/j.1600-0889.2010.00485, 2010.

Crevoisier, C., Sweeney, C., and Gloor, M.: Regional US carbon sinks from three-dimensional atmospheric CO_2 sampling, P. Natl. Acad. Sci. USA, 107, 43, 18348–18353, doi:10.1073/pnas.0900062107, 2010.

DeFries, R. and Townshend, J. R.: NDVI-derived land cover classifications at a global scale, Int. J. Remote Sens., 37–41, doi:10.1080/01431169408954345, 1994.

Deng, F. and Chen, J. M.: Recent global CO_2 flux inferred from atmospheric CO_2 observations and its regional analyses, Biogeosciences, 8, 3263–3281, doi:10.5194/bg-8-3263-2011, 2011.

Deng, F., Chen, J. M., and Plummer, S.: Algorithm for global leaf area index retrieval using satellite imagery, IEEE T. Geosci. Remote, 44, 2219–2229, 2006.

Deng, F., Chen, J. M., Ishizawa, M., Yuen, C.-W., Mo, G., Higuchi, K., Chan, D., Chen, B., and Maksyutov, S.: Global monthly CO_2 flux inversion with a focus over North America, Tellus B, 59, 179–190, doi:10.1111/j.1600-0889.2006.00235, 2007.

Deng, F., Chen, J. M., Pan, Y., Peters, W., Birdsey, R., McCullough, K., and Xiao, J.: The use of forest stand age information in an atmospheric CO_2 inversion applied to North America, Biogeosciences, 10, 5335–5348, doi:10.5194/bg-10-5335-2013, 2013.

Denning, A. S., Fung, I. Y., and Randall, D.: Latitudinal gradient of atmospheric CO_2 due to seasonal exchange with land biota, Nature, 376, 240–243, doi:10.1038/376240a0, 1995.

Enting, I. G.: Inverse Problems in Atmospheric Constituent Transport, Carbon, Cambridge University Press„ doi:10.1017/CBO9780511535741, 2002.

Enting, I. and Trudinger, C.: A synthesis inversion of the concentration and $\delta^1$3C of atmospheric CO_2, Tellus B, doi:10.1034/j.1600-0889.47, 1995.

Fan, S.: A large terrestrial carbon sink in North America implied by atmospheric and oceanic carbon dioxide data and models, Science, 282, 442–446, doi:10.1126/science.282.5388.442, 1998.

Gourdji, S. M., Mueller, K. L., Yadav, V., Huntzinger, D. N., Andrews, A. E., Trudeau, M., Petron, G., Nehrkorn, T., Eluszkiewicz, J., Henderson, J., Wen, D., Lin, J., Fischer, M.,

BGD
11, 6069–6117, 2014

Sweeney, C., and Michalak, A. M.: North American CO_2 exchange: inter-comparison of modeled estimates with results from a fine-scale atmospheric inversion, Biogeosciences, 9, 457–475, doi:10.5194/bg-9-457-2012, 2012.

Gurney, K. R., Law, R. M., Denning, A. S., Rayner, P. J., Baker, D., Bousquet, P., Bruhwiler, L. Chen, Y.H. , Ciais, P., Fan, S., Fung, I. Y., Gloor, M., Heimann, M., Higuchi, K., John, J., Maki, T., Maksyutov, S., Masarie, K., Peylin, P., Prather, M., Pak, B. C., Randerson, J., Sarmiento, J., Taguchi, S., Takahashi, T., and Yuen, C. W.: Towards robust regional estimates of CO_2 sources and sinks using atmospheric transport models, Nature, 415, 626–30, doi:10.1038/415626a, 2002.

Gurney, K. R., Law, R. M., Denning, A. S., Rayner, P. J., Baker, D., Bousquet, P., Bruhwiler, L., De Jong, B. H., McConkey, B. G., Birdsey, R., Kurz, W. A., Jacobson, A. R., Huntzinger, D. N., Pan, Y., Post, W. M., and Cook, R. B.: TransCom 3 CO_2 inversion intercomparison: 1. Annual mean control results and sensitivity to transport and prior flux information, Tellus B, 55, 555–579, doi:/10.1034/j.1600-0889.2003.00049.x/full, 2003.

Gurney, K. R., Law, R. M., Denning, A. S., Rayner, P. J., Pak, B. C., Baker, D., Bousquet, P., Bruhwiler, L., Chen, Y.-H., Ciais, P., Fung, I. Y., Heiman, M., John, J., Maki, T., Maksyutov, S., Peylin, P., Prather, M., and Taguchi, S.: Transcom 3 inversion intercomparison: model mean results for the estimation of seasonal carbon sources and sinks, Global Biogeochem. Cy., 18, doi:10.1029/2003GB002111, 2004.

Hayes, D. J., Turner, D. P., Stinson, G., McGuire, A. D., Wei, Y., West, T. O., Heath, L. S.Saha, S., White, G., Woollen, J., Zhu, Y., Leetmaa, A., Reynolds, B., Chelliah, M., Ebisuzaki, W., Higgins, W., Janowiak, J., Mo, K. C., Ropelewski, C., Wang, J., Jenne, R., and Joseph, D.: Reconciling estimates of the contemporary North American carbon balance among terrestrial biosphere models, atmospheric inversions, and a new approach for estimating net ecosystem exchange from inventory-based data, Glob. Change Biol., 18, 1282–1299, doi:10.1111/j.1365-2486.2011.02627, 2012.

He, L., Chen, J. M., Pisek, J., Schaaf, C. B., and Strahler, A. H.: Global clumping index map derived from the MODIS BRDF product, Remote Sens. Environ., 119, 118–130, 2012.

Hicke, J. A.: Spatiotemporal patterns of cropland area and net primary production in the central United States estimated from USDA agricultural information, Geophys. Res. Lett., 31, 1–5, doi:10.1029/2004GL020927, 2004.

BGD
11, 6069–6117, 2014

Hicke, J. A. and Lobell, D.: Cropland area and net primary production computed from 30 years of USDA agricultural harvest data, Earth Interact., 8,doi:10.1175/1087-3562(2004)008<0001:CAANPP>2.0.CO;2, 2004.
Higuchi, K., Shashkov, A., Chan, D., Saigusa, N., Murayama, S., Yamamoto, S., Kondo, H., Chen, J. M., Liu, J., and Chen, B.: Simulations of seasonal and inter-annual variability of gross primary productivity at Takayama with BEPS ecosystem model, Agr. Forest Meteorol., 134, 143–150, doi:10.1016/j.agrformet.2005.08.018, 2005.
Huntzinger, D. N., Post, W. M., Wei, Y., Michalak, A. M., West, T. O., Jacobson, A. R., Baker, I. T. Chen, J., Davis, K., Hayes, D., Hoffman, F., Jain, A., Liu, S., McGuire, A., Neilson, R., Potter, C., Poulter, B., Price, D., Raczka, B., Tian, H., Thornton, P., Tomelleri, E., Viovy, N., Xiao, J., Yuan, W., Zeng, N., Zhao, M., and Cook. R.: North American Carbon Program (NACP) regional interim synthesis: terrestrial biospheric model intercomparison, Ecol. Model., 232, 144–157, doi:10.1016/j.ecolmodel.2012.02.004, 2012.
Ju, W., Chen, J. M., Black, T. A., Barr, A. G., Liu, J., and Chen, B.: Modelling multi-year coupled carbon and water fluxes in a boreal aspen forest, Agr. Forest Meteorol., 140, 136–151, doi:10.1016/j.agrformet.2006.08.008, 2006.
Kalnay, E., Kanamitsu, M., Kistler, R., Collins, W., Deaven, D., Gandin, L., Iredell, M. Saha, S., White, G., Woollen, J., Zhu, Y., Leetmaa, A., Reynolds, B., Chelliah, M., Ebisuzaki, W., Higgins, W., Janowiak, J., Mo, K. C., Ropelewski, C., Wang, J., Jenne, R., and Joseph, D.: The NCEP/NCAR 40 year reanalysis project, B. Am. Meteorol. Soc., 77, 437–471, doi:10.1175/1520-0477(1996)077<0437:TNYRP>2.0.CO;2, 1996.
Krol, M., Houweling, S., Bregman, B., van den Broek, M., Segers, A., van Velthoven, P., Peters, W., Dentener, F., and Bergamaschi, P.: The two-way nested global chemistry-transport zoom model TM5: algorithm and applications, Atmos. Chem. Phys., 5, 417–432, doi:10.5194/acp-5-417-2005, 2005.
Kurz, W. A. and Apps, M. J.: A 70 year retrospective analysis of carbon fluxes in the Canadian forest sector, Ecol. Appl., 9, 526–547, 1999.
Lauvaux, T., Schuh, A. E., Uliasz, M., Richardson, S., Miles, N., Andrews, A. E., Sweeney, C., Diaz, L. I., Martins, D., Shepson, P. B., and Davis, K. J.: Constraining the CO_2 budget of the corn belt: exploring uncertainties from the assumptions in a mesoscale inverse system, Atmos. Chem. Phys., 12, 337–354, doi:10.5194/acp-12-337-2012, 2012.
Le Quéré, C., Raupach, M. R., Canadell, J. G., Marland, G., Bopp, L., Ciais, P., Conway, T. J. Doney, S. C., Feely, R. A., Foster, P. N., Friedlingstein, P., Gurney, K., Houghton, R. A., House,

BGD
11, 6069–6117, 2014

J. I., Huntingford, C., Levy, P. E., Lomas, M. R., Majkut, J., Metzl, N., Ometto, J. P., Peters, G. P., Prentice, I. C., Randerson, J. T., Running, S. W., Sarmiento, J. L., Schuster, U., Sitch, S., Takahashi, T., Viovy, N., van der Werf, G. R., and Woodward, F. I.: Trends in the sources and sinks of carbon dioxide, Nat. Geosci., 2, 831–836, doi:10.1038/ngeo689, 2009.

Le Quéré, C., Andres, R. J., Boden, T., Conway, T., Houghton, R. A., House, J. I., Marland, G., Peters, G. P., van der Werf, G. R., Ahlström, A., Andrew, R. M., Bopp, L., Canadell, J. G., Ciais, P., Doney, S. C., Enright, C., Friedlingstein, P., Huntingford, C., Jain, A. K., Jourdain, C., Kato, E., Keeling, R. F., Klein Goldewijk, K., Levis, S., Levy, P., Lomas, M., Poulter, B., Raupach, M. R., Schwinger, J., Sitch, S., Stocker, B. D., Viovy, N., Zaehle, S., and Zeng, N.: The global carbon budget 1959–2011, Earth Syst. Sci. Data, 5, 165–185, doi:10.5194/essd-5-165-2013, 2013.

Liu, J., Chen, J. M., Cihlar, J., and Chen, W.: Net primary productivity distribution in the BOREAS region from a process model using satellite and surface data, J. Geophys. Res., 104, 27735–27754, 1999.

Liu, J., Chen, J. M., Cihlar, J., and Chen, W.: Net primary productivity mapped for Canada at 1 km resolution, Global Ecol. Biogeogr., 11, 115–129, 2002.

Madec, G., Delecluse, P., Imbard, M., and Levy, C.: OPA 8.1 Ocean General Circulation Model reference manual, 11. Notes du pôle de modélisation Institut Pierre Simon Laplace IPSL France, 11, 91 pp., 1998.

Marland, G., Hamal, K., and Jonas, M.: How uncertain are estimates of CO_2 emissions?, J. Ind. Ecol., 13, 4–7, doi:10.1111/j.1530-9290.2009.00108, 2009.

Masarie, K. and Tans, P. P.: Extension and integration of atmospheric carbon dioxide data into a globally consistent measurement record, J. Geophys. Res., 100, 11593–11610, 1995.

Matsushita, B. and Tamura, M.: Integrating remotely sensed data with an ecosystem model to estimate net primary productivity in East Asia, Remote Sens. Environ., 81, 58–66, 2002.

Olivier, J. and Aardenne, J. V.: Recent trends in global greenhouse gas emissions?: Regional trends 1970–2000 and spatial distribution of key sources in 2000, Environm. Sci., 2, 81–99, 2005.

Pacala, S., Hurtt, G., Baker, D., and Peylin, P.: Consistent land- and atmosphere-based US carbon sink estimates, Science, available at: http://www.sciencemag.org/content/292/5525/2316.short, 2001.

Pan, Y., Birdsey, R. A., Fang, J., Houghton, R. A., Kauppi, P. E., Kurz, W. A., Phillips, O. L. Shvidenko, A., Lewis, S. L., Canadell, J. G., Ciais, P., Jackson, R. B., Pacala, S. W., McGuire,

BGD
11, 6069–6117, 2014

A. D., Piao, S., Rautiainen, A., Sitch, S., and Hayes, D.: A large and persistent carbon sink in the World's forests, Science, 333, 988–993, 2011a.

Pan, Y., Chen, J. M., Birdsey, R., McCullough, K., He, L., and Deng, F.: Age structure and disturbance legacy of North American forests, Biogeosciences, 8, 715–732, doi:10.5194/bg-8-715-2011, 2011b.

Peters, W., Miller, J. B., Whitaker, J., Denning, A. S., Hirsch, A., Krol, M. C., Zupanski, D., Bruhwiler, L., and Tans, P. P.: An ensemble data assimilation system to estimate CO_2 surface fluxes from atmospheric trace gas observations, J. Geophys. Res., 110, D24304, doi:10.1029/2005JD006157, 2005.

Peters, W., Jacobson, A. R., Sweeney, C., Andrews, A. E., Conway, T. J., Masarie, K., Miller, J. B., Bruhwiler, L. M. P., Petron, G., Hirsch, A. I., Worthy, D. E. J., van der Werf, G. R., Randerson, J. T., Wennberg, P. O., Krol, M. C., and Tans, P. P.: An atmospheric perspective on North American carbon dioxide exchange: CarbonTracker, P. Natl. Acad. Sci. USA, 104, 18925–18930, doi:10.1073/pnas.0708986104, 2007.

Peylin, P., Law, R. M., Gurney, K. R., Chevallier, F., Jacobson, A. R., Maki, T., Niwa, Y., Patra, P. K., Peters, W., Rayner, P. J., Rödenbeck, C., van der Laan-Luijkx, I. T., and Zhang, X.: Global atmospheric carbon budget: results from an ensemble of atmospheric CO_2 inversions, Biogeosciences, 10, 6699–6720, doi:10.5194/bg-10-6699-2013, 2013.

Prince, S. D., Haskett, J., Steininger, M., Strand, H., and Wright, R.: Net primary production of US Midwest croplands from agricultural harvest yield data, Ecol. Appl., 11, 1194–1205, 2001.

Randerson, J. T., Thompson, V., Conway, T. J., Fung, I. Y., and Field, B.: The contribution of terrestrial sources and sinks to trends in the seasonal cycle of atmospheric carbon dioxide, Global Biogeochem. Cy., 11, 535–560, 1997.

Randerson, J. T., Van Der Werf, G. R., Giglio, L., Collatz, G. J., and Kasibhatla, P. S.: Global Fire Emissions Database, Version 2 (GFEDv2.1), Data Set, available online, Oak Ridge National Laboratory Distributed Active Archive Center, Oak Ridge, Tennessee, USA, 2007.

Running, S. W. and Coughlan, J. C.: A general model of forest ecosystem processes for regional applications, I. Hydrologic balance, canopy gas exchange and primary production processes, Ecol. Model., 42, 125–154, 1988.

Rödenbeck, C., Houweling, S., Gloor, M., and Heimann, M.: CO_2 flux history 1982–2001 inferred from atmospheric data using a global inversion of atmospheric transport, Atmos. Chem. Phys., 3, 1919–1964, doi:10.5194/acp-3-1919-2003, 2003.

BGD
11, 6069–6117, 2014

Schuh, A. E., Lauvaux, T., West, T. O., Denning, S., Davis, K., Miles, N., Richardson, S., Uliasz, M., Lokupitiya, E., Cooley, S., Andrews, A., and Ogle, S.: Evaluating atmospheric CO_2 inversions at multiple scales over a highly inventoried agricultural landscape, Glob. Change Biol., 19, 1424–1439, doi:10.1111/gcb.12141, 2013.

Sun, R., Chen, J., Zhu, Q., Zhou, Y., and Liu, J.: Spatial distribution of net primary productivity and evapotranspiration in Changbaishan Natural Reserve, China, using Landsat ETM+ data, Can. J. Remote Sens., 30, 731–742, 2004.

Tarantola, A.: Inverse Problem Theory, Siam edn., Physica B: Condensed Matter, Vol. 130, 77–78, SIAM, doi:10.1137/1.9780898717921, 2005.

Turner, D. P., Jacobson, A. R., Ritts, W. D., Wang, W. L., and Nemani, R.: A large proportion of North American net ecosystem production is offset by emissions from harvested products, river/stream evasion, and biomass burning, Glob. Change Biol., 19, 3516–3528, doi:10.1111/gcb.12313, 2013.

Webb, R. S., Rosenzweig, C. E., and Levine, E. R.: A Global Data Set of Soil Particle Size Properties, NASA Tech. Memo., TM-4286, NASA, USA, 40 pp., 1991.

West, T. O., Brandt, C. C., Wilson, B. S., Hellwinckel, C. M., Tyler, D. D., Marland, G., De La Torre Ugarte, D. G., Larson, J. A., and Nelson, R.: Estimating regional changes in soil carbon with high spatial resolution, Soil Sci. Soc. Am. J., 72, 285, doi:10.2136/sssaj2007.0113, 2008.

West, T. O., Marland, G., Singh, N., Bhaduri, B. L., and Roddy, A. B.: The human carbon budget: an estimate of the spatial distribution of metabolic carbon consumption and release in the United States, Biogeochemistry, 94, 29–41, doi:10.1007/s10533-009-9306-z, 2009.

West, T. O., Brandt, C. C., Baskaran, L. M., Hellwinckel, C. M., Mueller, R., Bernacchi, C. J., Bandaru, V., Yang, B., Wilson, B. S., Marland, G., Nelson, R. G., De La Torre Ugarte, D. G., and Post, W. M.: Cropland carbon fluxes in the United States: increasing geospatial resolution of inventory-based carbon accounting, Ecol. Appl., 20, 1074–1086, 2010.

West, T. O., Bandaru, V., Brandt, C. C., Schuh, A. E., and Ogle, S. M.: Regional uptake and release of crop carbon in the United States, Biogeosciences, 8, 2037–2046, doi:10.5194/bg-8-2037-2011, 2011.

Williams, C. A., Collatz, G. J., Masek, J., and Goward, S. N.: Carbon consequences of forest disturbance and recovery across the conterminous United States, Global Biogeochem. Cy., 26, GB1005, doi:10.1029/2010GB003947, 2012.

BGD
11, 6069–6117, 2014

Yuen, C.-W.: Impact of Fraserdale CO_2 observations on annual flux inversion of the North American boreal region, Tellus B, 203–209, doi:/10.1111/j.1600-0889.2005.00150, 2005.
van der Werf, G. R., Randerson, J. T., Giglio, L., Collatz, G. J., Kasibhatla, P. S., and Arellano Jr., A. F.: Interannual variability in global biomass burning emissions from 1997 to 2004, Atmos. Chem. Phys., 6, 3423–3441, doi:10.5194/acp-6-3423-2006, 2006.
van der Werf, G. R., Randerson, J. T., Giglio, L., Collatz, G. J., Mu, M., Kasibhatla, P. S., Morton, D. C., DeFries, R. S., Jin, Y., and van Leeuwen, T. T.: Global fire emissions and the contribution of deforestation, savanna, forest, agricultural, and peat fires (1997–2009), Atmos. Chem. Phys., 10, 11707–11735, doi:10.5194/acp-10-11707-2010, 2010.
Zhang, F. M., Chen, J. M., Birdsey, R. A., Pan, Y., Shen, S., Ju, W. J., and He, L.: Attributing carbon changes in conterminous US forests to disturbance and non-disturbance factors from 1901 to 2010, J. Geophys. Res.-Biogeo., 117, G02021, doi:10.1029/2011JG001930, 2012.

BGD
11, 6069–6117, 2014

Table 1. Summary of background prior fluxes and their uncertainties.

Background flux	Data source	Temporal variability	Uncertainty
Fossil Fuel	CDIAC (Marland et al., 2009) + EDGAR 4 database (Olivier and Aardenne, 2005)	Interannual	n/a
Fire	GFEDv2 (Randerson et al., 2007)	Interannual	n/a
Biosphere	BEPS model (Chen et al., 2003; Ju et al., 2006)	Interannual, seasonal, diurnal	2.0 $PgCyr^{-1}$ (Gurney et al., 2003) distributed globally over land surfaces regions based on spatial pattern of the GPP
Ocean	OPA-PISCES-T model (Buitenhuis et al., 2006)	Seasonal	0.67 $PgCyr^{-1}$ distributed over ocean regions (Deng and Chen, 2011)

BGD
11, 6069–6117, 2014

Table 2. Schemes of experiments designed to test for the impact of integrating information from crop production and consumption data into the a priorifluxes.

Experiment 1.	Annually balanced terrestrial biosphere	χ^2
(a)	Neutralized terrestrial prior fluxes from BEPS model (annual mean = 0)	1.09
(b)	Neutralized terrestrial prior fluxes (annual mean = 0) adjusted for crop production	1.12
(c)	Neutralized terrestrial prior fluxes (annual mean = 0) adjusted for crop production and crop consumption (added to the prior fluxes as a source)	0.97
Experiment 2.	Interannual variability in terrestrial biosphere	χ^2
(a)	Terrestrial prior fluxes from BEPS model (annual mean $\neq$ 0)	1.11
(b)	Terrestrial prior fluxes (annual mean $\neq$ 0) adjusted for crop production	1.16
(c)	Terrestrial prior fluxes (annual mean $\neq$ 0) adjusted for crop production and crop consumption	0.97

BGD
11, 6069–6117, 2014

Table 3. 2002 to 2007 mean inverted CO_2 flux (μ), the error (ε) in Tg C yr^{-1} and the percentage change (Δ %) for global regions. * represents regions with SNR > 1, and +ve percentage change in Δ % represents increase in uptake. West includes Regions 18, 19, 23, 24, and 25; Midwest includes Regions 20 and 21; Northeast includes Region 22, and Southeast includes regions 26, 27, and 28.

Region	Experiment 1					Experiment 2				
	(a)	(b)		(c)		(a)	(b)		(c)	
	$\mu \pm \varepsilon$	$\mu \pm \varepsilon$	Δ%	$\mu \pm \varepsilon$	Δ%	$\mu \pm \varepsilon$	$\mu \pm \varepsilon$	Δ%	$\mu \pm \varepsilon$	Δ%
18	−43.27 ± 33.1	−27.56 ± 25.7	−36.31	−23.35 ± 28.4	−46.03	−26.48 ± 33.1	−18.95 ± 25.7	−28.43	−14.74 ± 28.4	−44.32
19	−10.80 ± 20.3	−6.44 ± 15.8	−40.36	−2.67 ± 17.7	−75.26	−15.22 ± 20.3	−17.18 ± 15.8	12.88	−13.41 ± 17.7	−11.87
20	−71.59 ± 56.9	−208.50 ± 91.4	191.26*	−212.88 ± 102.4	197.38*	−113.85 ± 56.9	−227.33 ± 91.4	99.67*	−231.71 ± 102.4	103.52*
21	−117.07 ± 59.8	−153.83 ± 72.7	31.40	−149.69 ± 78.3	27.87	−132.20 ± 59.8	−192.76 ± 72.7	45.81	−188.63 ± 78.3	42.68
22	−104.91 ± 57.7	−84.51 ± 46.1	−19.45	−73.14 ± 51.9	−30.28	−145.62 ± 57.7	−124.70 ± 46.1	−14.36	−113.33 ± 51.9	−22.17
23	−0.79 ± 8.9	−0.26 ± 7.0	−67.39	6.63 ± 10.2	−941.50*	1.66 ± 8.9	0.34 ± 7	−79.75	7.23 ± 10.2	334.19
24	−0.05 ± 0.0	−1.01 ± 0.0	1796.23*	3.81 ± 3.5	−7286.79*	−3.00 ± 0.0	−4.93 ± 0.0	64.71*	−0.12 ± 3.5	−96.03
25	−7.95 ± 14.2	−6.98 ± 10.9	−12.23	−0.59 ± 14.2	−92.61	−23.48 ± 14.2	−26.09 ± 10.9	11.12	−19.70 ± 14.2	−16.10
26	−92.88 ± 59.8	−81.72 ± 47.5	−12.02	−56.41 ± 63.8	−39.27	−160.95 ± 59.8	−138.33 ± 47.5	−14.06	−113.01 ± 63.8	−29.79
27	−111.07 ± 78.7	−107.69 ± 64.6	−3.05	−81.40 ± 82.9	−26.72	−175.18 ± 78.7	−167.96 ± 64.6	−4.12	−141.68 ± 82.9	−19.12
28	−69.17 ± 67.5	−56.57 ± 51.0	−18.22	−31.80 ± 64.5	−54.02	−76.25 ± 67.5	−63.05 ± 51.0	−17.30	−38.29 ± 64.5	−49.78
West	−62.85 ± 39.1	−42.24 ± 30.4	−32.8	−16.17 ± 32.7	−74.28*	−66.50 ± 40.2	−66.81 ± 20.6	0.46	−40.75 ± 23.4	−38.73*
Midwest	−188.65 ± 80.7	−362.32 ± 116.8	92.06*	−362.57 ± 128.8	92.19*	−246.05 ± 82.3	−420.09 ± 115.5	70.73*	−420.33 ± 128.2	70.83*
Northeast	−104.91 ± 57.7	−84.51 ± 46.1	−19.45	−91.12 ± 51.9	−13.14	−145.62 ± 57.7	−124.70 ± 46.1	−14.36	−131.31 ± 51.9	−9.82
Southeast	−273.13 ± 118.2	−245.97 ± 94.2	−9.94	−169.61 ± 119.3	−37.90	−412.38 ± 115.5	−369.34 ± 93.1	−10.44	−292.98 ± 119.4	−28.95
US	−629.54 ± 157.7	−735.04 ± 153.9	16.76	−624.46 ± 172.7	−0.81	−870.55 ± 156.3	−980.94 ± 152.2	12.68	−885.37 ± 182.4	1.70
Canada	−295.59 ± 142.8	−258.04 ± 139.5	−12.70	−270.77 ± 139.7	−8.40	−255.50 ± 137.2	−219.74 ± 136.7	−14.00	−217.45 ± 136.3	−14.89
NA	−932.61 ± 205.9	−988.03 ± 195.9	5.94	−892.16 ± 211.4	−4.34	−1139.67 ± 189.9	−1206.04 ± 181.8	5.82	−1110.17 ± 200.3	−2.59

BGD
11, 6069–6117, 2014

Table 4. Correlation coefficients of the change in the inverted flux from Experiments 2a to Experiment 2c among 11 regions in USA, calculated based on inverted annual fluxes in 2000–2007.

Region	18	19	20	21	22	23	24	25	26	27	28
18	1	0.88	−0.57	−0.56	0.33	0.13	−0.16	0.55	0.09	0.16	0.75
19	0.88	1	−0.54	−0.69	0.43	0.29	0.02	0.72	0.17	0.16	0.70
20	−0.57	−0.54	1	0.06	−0.36	−0.34	0.12	−0.01	−0.46	−0.21	−0.19
21	−0.56	−0.69	0.06	1	−0.48	0.10	0.10	−0.78	−0.44	−0.25	−0.71
22	0.33	0.43	−0.36	−0.48	1	−0.18	−0.45	0.12	0.61	0.09	−0.01
23	0.13	0.29	−0.34	0.10	−0.18	1	0.87	0.41	−0.14	0.67	0.23
24	−0.16	0.02	0.12	0.10	−0.45	0.87	1	0.41	−0.27	0.63	0.16
25	0.55	0.72	−0.01	−0.78	0.12	0.41	0.41	1	−0.03	0.46	0.86
26	0.09	0.17	−0.46	−0.44	0.61	−0.14	−0.27	−0.03	1	0.29	−0.03
27	0.16	0.16	−0.21	−0.25	0.09	0.67	0.63	0.46	0.29	1	0.37
28	0.75	0.70	−0.19	−0.71	−0.01	0.23	0.16	0.86	−0.03	0.37	1

BGD
11, 6069–6117, 2014

Table 5. 2002 to 2007 mean inverted CO_2 flux (μ), the error (ε) in $PgC\,yr^{-1}$ and the percentage change (Δ%) for global regions. * represents regions with SNR > 1, and +ve percentage change in Δ %, represents increase in uptake/release.

Region	Experiment 1					Experiment 2				
	(a)	(b)		(c)		(a)	(b)		(c)	
	$\mu \pm \varepsilon$	$\mu \pm \varepsilon$	Δ%	$\mu \pm \varepsilon$	Δ%	$\mu \pm \varepsilon$	$\mu \pm \varepsilon$	Δ%	$\mu \pm \varepsilon$	Δ%
NA-N	−0.28 ± 0.14	−0.24 ± 0.14	−13.01	−0.26 ± 0.14	−7.57	−0.22 ± 0.14	−0.18 ± 0.14	−14.89	−0.20 ± 0.14	−7.83
NA-S	−0.65 ± 0.16	−0.74 ± 0.16	14.07	−0.63 ± 0.16	−2.95	−0.92 ± 0.16	−1.02 ± 0.16	10.65	−0.91 ± 0.19	−1.37
31	0.36 ± 0.41	0.35 ± 0.41	−0.61	0.34 ± 0.41	−5.59	0.34 ± 0.41	0.39 ± 0.41	14.34	0.37 ± 0.41	9.12
32	−0.07 ± 0.27	−0.07 ± 0.27	−3.62	−0.06 ± 0.27	−10.04	−0.11 ± 0.27	−0.09 ± 0.27	−16.89	−0.08 ± 0.27	−21.02
33	−0.20 ± 0.28	−0.19 ± 0.28	−5.45	−0.22 ± 0.28	8.30	−0.28 ± 0.28	−0.19 ± 0.28	−33.92	−0.22 ± 0.28	−24.07
34	−0.86 ± 0.27	−0.86 ± 0.27	−0.15	−0.86 ± 0.27	−0.63	−0.93 ± 0.27	−0.91 ± 0.27	−2.33	−0.91 ± 0.27	−2.78
35	−0.90 ± 0.26	−0.87 ± 0.26	−2.97	−0.89 ± 0.26	−0.40	−1.00 ± 0.26	−0.96 ± 0.26	−3.73	−0.99 ± 0.26	−1.42
36	−0.63 ± 0.24	−0.61 ± 0.24	−3.34	−0.64 ± 0.24	0.57	−0.52 ± 0.24	−0.54 ± 0.24	4.97	−0.57 ± 0.24	9.75
37	−0.54 ± 0.24	−0.54 ± 0.24	0.57	−0.54 ± 0.24	0.78	−0.63 ± 0.24	−0.59 ± 0.24	−7.49	−0.59 ± 0.24	−7.32
38	0.06 ± 0.08	0.06 ± 0.08	1.05	0.06 ± 0.08	1.91	0.04 ± 0.08	0.04 ± 0.08	−2.77	0.04 ± 0.08	−1.58
39	−0.21 ± 0.21	−0.18 ± 0.21	−14.44	−0.19 ± 0.21	−7.45	−0.06 ± 0.21	−0.01 ± 0.21	−88.22	−0.02 ± 0.21	−64.84
40	−0.58 ± 0.15	−0.58 ± 0.15	1.22	−0.59 ± 0.15	3.00	−0.62 ± 0.15	−0.63 ± 0.15	1.22	−0.64 ± 0.15	2.87
41	−0.06 ± 0.12	−0.07 ± 0.12	10.86	−0.06 ± 0.12	2.11	0.00 ± 0.12	−0.01 ± 0.12	138.30	0.00 ± 0.12	−45.39
42	0.74 ± 0.14	0.74 ± 0.14	−0.72	0.74 ± 0.14	−0.14	0.80 ± 0.14	0.79 ± 0.14	−0.90	0.79 ± 0.14	−0.36
43	−0.58 ± 0.18	−0.58 ± 0.18	0.25	−0.58 ± 0.18	−0.35	−0.51 ± 0.18	−0.51 ± 0.18	0.77	−0.51 ± 0.18	0.08
44	−0.27 ± 0.07	−0.28 ± 0.07	2.85	−0.27 ± 0.07	1.07	−0.27 ± 0.07	−0.28 ± 0.07	3.52	−0.28 ± 0.07	1.76
45	−0.34 ± 0.12	−0.34 ± 0.12	−0.84	−0.36 ± 0.12	4.30	−0.31 ± 0.12	−0.30 ± 0.12	−3.08	−0.32 ± 0.12	2.52
46	0.10 ± 0.12	0.10 ± 0.12	−0.60	0.10 ± 0.12	−0.41	0.15 ± 0.12	0.15 ± 0.12	1.02	0.15 ± 0.12	1.14
47	−0.32 ± 0.14	−0.32 ± 0.14	−1.28	−0.32 ± 0.14	−1.52	−0.33 ± 0.14	−0.33 ± 0.14	−0.94	−0.33 ± 0.14	−1.18
48	0.15 ± 0.06	0.15 ± 0.06	−1.04	0.15 ± 0.06	−0.77	0.14 ± 0.06	0.14 ± 0.06	−0.73	0.14 ± 0.06	−0.45
49	0.06 ± 0.16	0.05 ± 0.16	−6.59	0.06 ± 0.16	−2.21	0.14 ± 0.16	0.14 ± 0.16	2.54	0.15 ± 0.16	4.36
50	−0.56 ± 0.13	−0.56 ± 0.13	−0.64	−0.56 ± 0.13	−0.87	−0.53 ± 0.13	−0.53 ± 0.13	−0.42	−0.53 ± 0.13	−0.66
Land	−3.93 ± 0.67	−3.89 ± 0.67	−0.83	−3.90 ± 0.65	−0.72	−4.30 ± 0.66	−4.07 ± 0.65	−5.39	−4.07 ± 0.66	−5.29
Oceans	−1.67 ± 0.37	−1.69 ± 0.37	1.43	−1.70 ± 0.37	1.70	−1.37 ± 0.38	−1.38 ± 0.37	0.98	−1.39 ± 0.37	1.31
Total	−5.59 ± 0.75	−5.59 ± 0.75	−0.16	−5.59 ± 0.74	0.01	−5.66 ± 0.75	−5.45 ± 0.74	−3.85	−5.46 ± 0.75	−3.70

BGD
11, 6069–6117, 2014

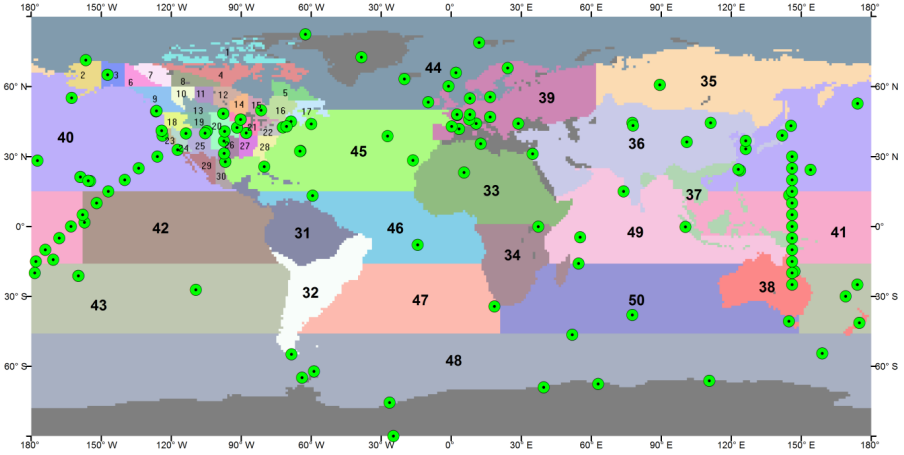

Fig. 1. A nested inversion system with 30 regions for North America and 20 regions for the remainder of the globe. The 210 measurement sites are indicated as circles.

BGD
11, 6069–6117, 2014

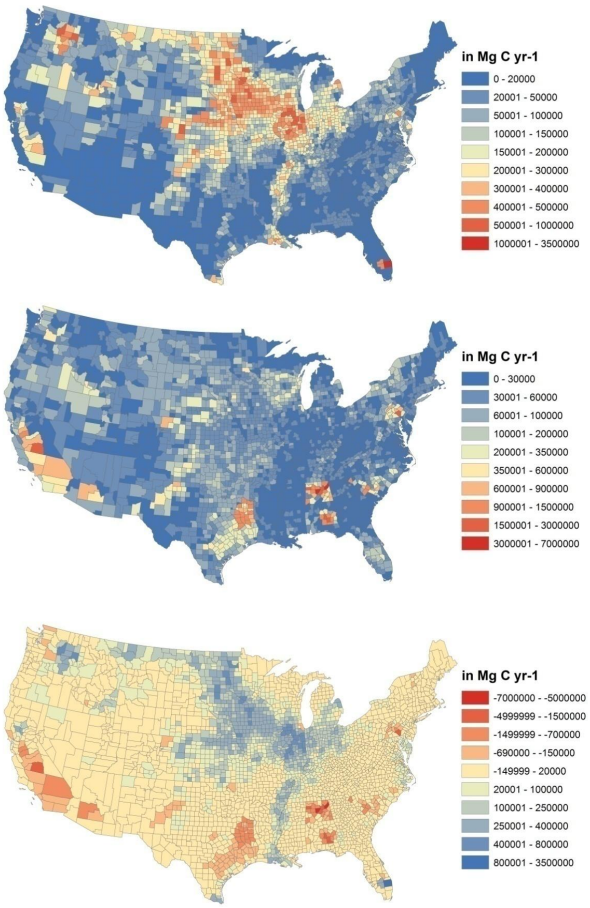

Fig. 2. Spatial distributions of annual crop production (top); crop consumption (middle); and crop NEP (bottom) for 2003. Data taken from (CDIAC) website: http://cdiac.ornl.gov.

BGD
11, 6069–6117, 2014

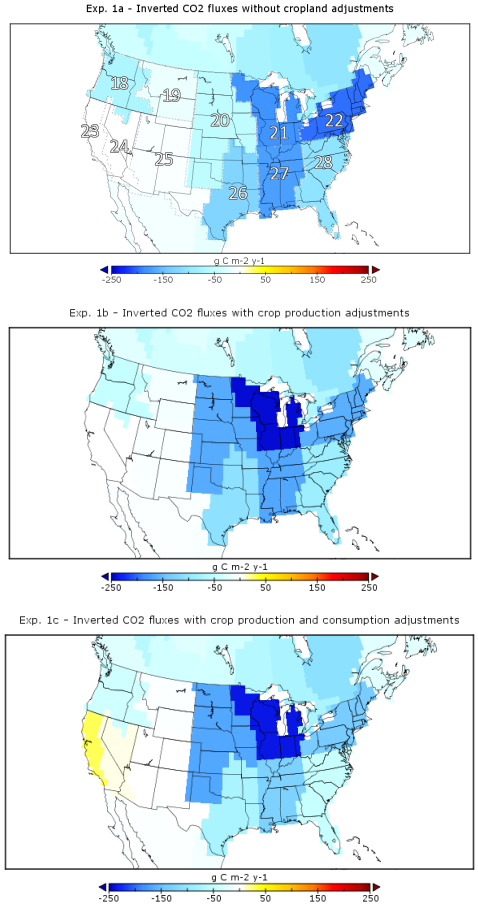

Fig. 3. Map of mean annual inverted CO_2 flux for Experiment 1 during 2002 to 2007 over contiguous US regions. Negative values represent carbon uptake.

BGD
11, 6069–6117, 2014

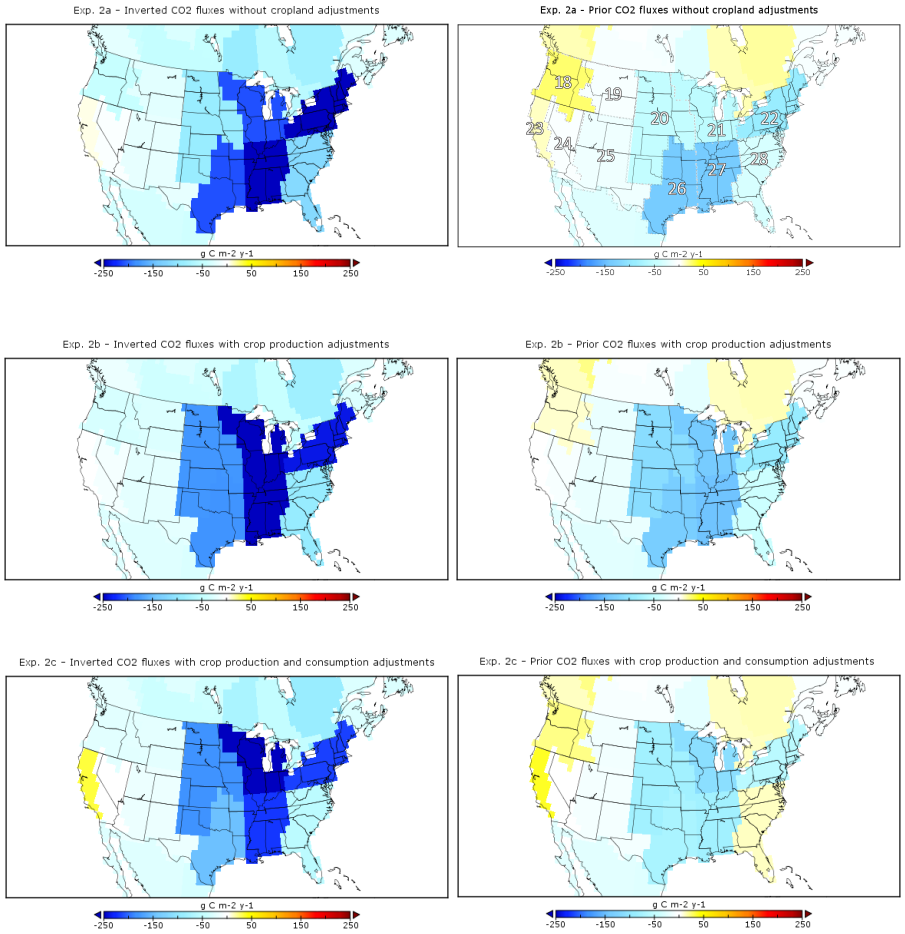

Fig. 4. Map of mean annual inverted (left) and prior (right) CO_2 flux for Experiment 2 during 2002 to 2007 over contiguous US. Negative values represent carbon uptake.

BGD
11, 6069–6117, 2014

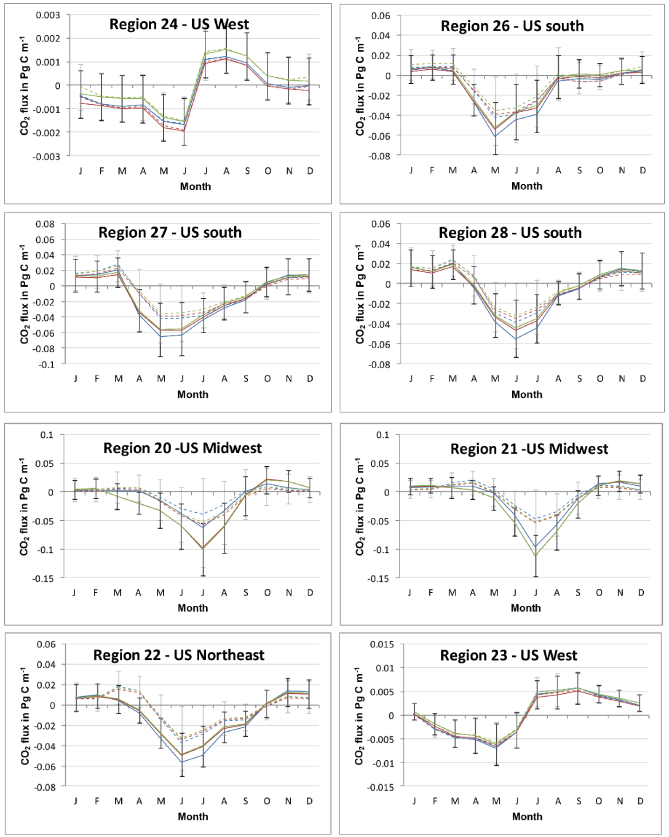

Fig. 5. Monthly inverted (solid lines) and prior (dashed lines) CO_2 flux (–ve represents uptake) averaged over 2002 to 2007 for Experiments 2 – annually varying terrestrial prior fluxes with **(a)** no adjustments – *blue*; **(b)** production adjustments – *red*; **(c)** crop production and consumption adjustments – *green*.

BGD
11, 6069–6117, 2014